図 6　（800-900m/z の部分を拡大）

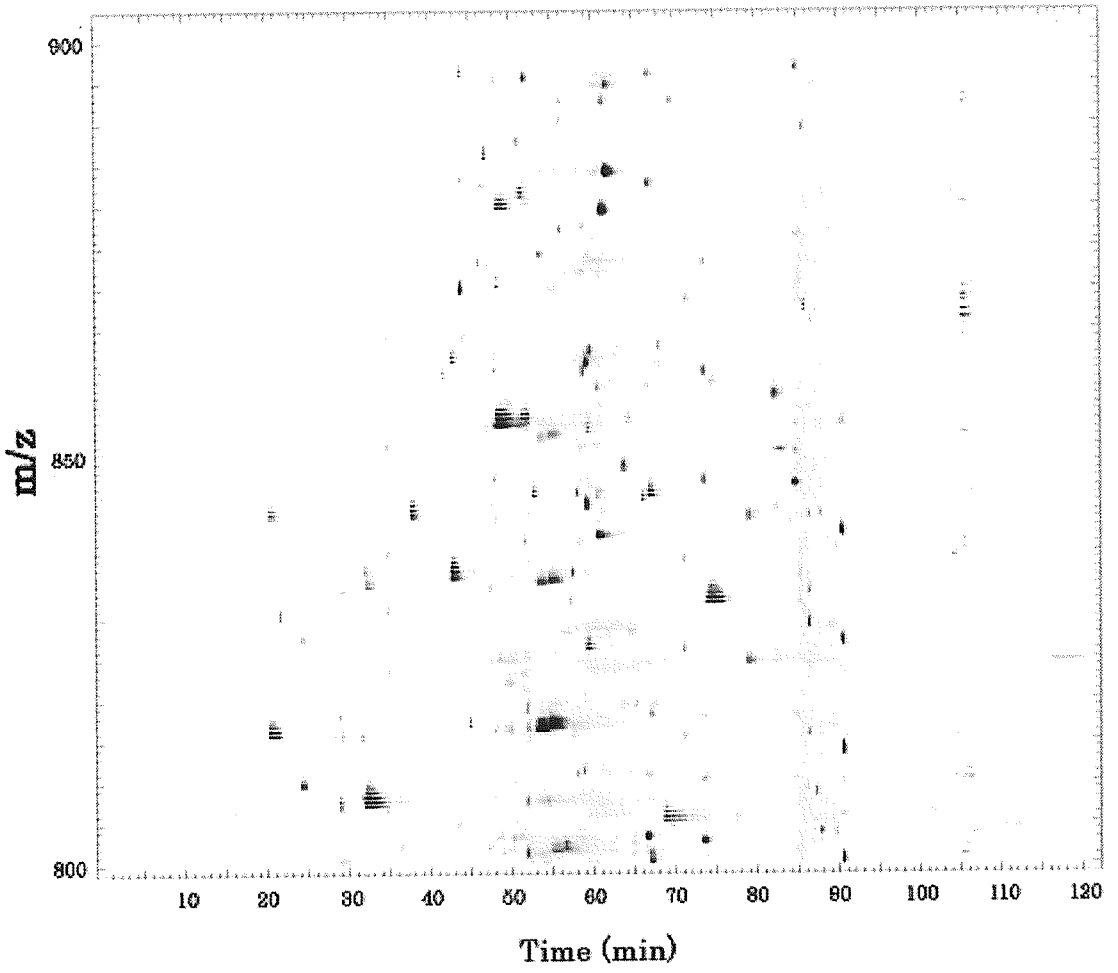


図 7　ICAT 解析の流れ

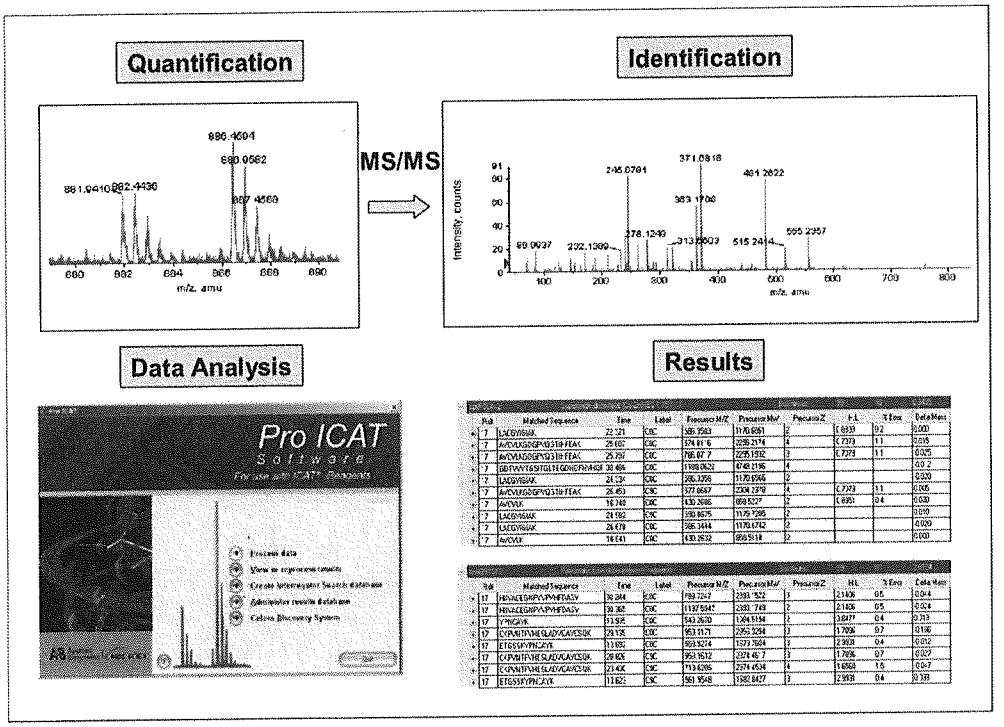

# 表1　ヒトプールド肝サイトゾル中でMASCOT検索により同定されたタンパク質

| NAME | ID | Description |
|---|---|---|
| CPSM_HUMAN | (P31327) | Carbamoyl-phosphate synthase [ammonia], mitochondrial precursor (EC 6.3.4.16) |
| ADHB_HUMAN | (P00325) | Alcohol dehydrogenase beta chain (EC 1.1.1.1) |
| ADH4_HUMAN | (P08319) | Alcohol dehydrogenase class II pi chain (EC 1.1.1.1) |
| ALDOB_HUMAN | (P05062) | Fructose-bisphosphate aldolase B (EC 4.1.2.13) (Liver-type aldolase) |
| ADHA_HUMAN | (P07327) | Alcohol dehydrogenase alpha chain (EC 1.1.1.1) |
| ADHG_HUMAN | (P00326) | Alcohol dehydrogenase gamma chain (EC 1.1.1.1) |
| G3P2_HUMAN | (P04406) | Glyceraldehyde-3-phosphate dehydrogenase, liver (EC 1.2.1.12) (GAPDH) |
| FABPL_HUMAN | (P07148) | Fatty acid binding protein, liver (L-FABP) |
| GSTA1_HUMAN | (P08263) | Glutathione S-transferase A1 (EC 2.5.1.18) (GTH1) (HA subunit 1) (GST-epsilon) (GSTA1-1) |
| ACTB_HUMAN | (P60709) | Actin, cytoplasmic 1 (Beta-actin) |
| ACTA_HUMAN | (P62736) | Actin, aortic smooth muscle (Alpha-actin-2) |
| HBB_HUMAN | (P68871) | Hemoglobin beta subunit (Hemoglobin beta chain) (Beta-globin) |
| GSTA2_HUMAN | (P09210) | Glutathione S-transferase A2 (EC 2.5.1.18) (GTH2) (HA subunit 2) (GST-gamma) (GSTA2-2) |
| HBA_HUMAN | (P69905) | Hemoglobin alpha subunit (Hemoglobin alpha chain) (Alpha-globin) |
| FTCD_HUMAN | (O95954) | Formimidoyltransferase-cyclodeaminase (Formiminotransferase-cyclodeaminase) (FTCD) (LCHC1) |
| DHE3_HUMAN | (P00367) | Glutamate dehydrogenase 1, mitochondrial precursor (EC 1.4.1.3) (GDH) |
| GSTA3_HUMAN | (Q16772) | Glutathione S-transferase A3-3 (EC 2.5.1.18) (GST class-alpha) |
| PRDX1_HUMAN | (Q06830) | Peroxiredoxin 1 (EC 1.11.1.15) (Thioredoxin peroxidase 2) (Thioredoxin-dependent peroxide |
| PRDX6_HUMAN | (P30041) | Peroxiredoxin 6 (EC 1.11.1.15) (Antioxidant protein 2) (1-Cys peroxiredoxin) (1-Cys PRX) |
| EF1A1_HUMAN | (P68104) | Elongation factor 1-alpha 1 (EF-1-alpha-1) (Elongation factor 1 A-1) (eEF1A-1) |
| ASSY_HUMAN | (P00966) | Argininosuccinate synthase (EC 6.3.4.5) (Citrulline--aspartate ligase) |
| DCXR_HUMAN | (Q7Z4W1) | L-xylulose reductase (EC 1.1.1.10) (XR) (Dicarbonyl/L-xylulose reductase) |
| ARGI1_HUMAN | (P05089) | Arginase-1 (EC 3.5.3.1) (Type I arginase) (Liver-type arginase) |
| ECHM_HUMAN | (P30084) | Enoyl-CoA hydratase, mitochondrial precursor (EC 4.2.1.17) (Short chain enoyl-CoA hydratas |
| FAS_HUMAN | (P49327) | Fatty acid synthase (EC 2.3.1.85) (Includes: [Acyl-carrier-protein] S-acetyltransferase |
| AL1A1_HUMAN | (P00352) | Retinal dehydrogenase 1 (EC 1.2.1.36) (RalDH1) (RALDH 1) (Aldehyde dehydrogenase family 1 |
| ST2A1_HUMAN | (Q06520) | Alcohol sulfotransferase (EC 2.8.2.2) (Hydroxysteroid sulfotransferase) (HST) |
| HMCS2_HUMAN | (P54868) | Hydroxymethylglutaryl-CoA synthase, mitochondrial precursor (EC 2.3.3.10) |
| IDHC_HUMAN | (O75874) | Isocitrate dehydrogenase [NADP] cytoplasmic (EC 1.1.1.42) (Oxalosuccinate decarboxylase) |
| PEBP_HUMAN | (P30086) | Phosphatidylethanolamine-binding protein (PEBP) (Prostate binding protein) (HCNPpp) |
| SODC_HUMAN | (P00441) | Superoxide dismutase [Cu-Zn] (EC 1.15.1.1) |
| PPIA_HUMAN | (P62937) | Peptidyl-prolyl cis-trans isomerase A (EC 5.2.1.8) (PPIase) (Rotamase) (Cyclophilin A) |
| AK1C1_HUMAN | (Q04828) | Aldo-keto reductase family 1 member C1 (EC 1.1.1.-) (20-alpha-hydroxysteroid dehydrogenase |
| CH60_HUMAN | (P10809) | 60 kDa heat shock protein, mitochondrial precursor (Hsp60) (60 kDa chaperonin) (CPN60) |
| ALDH2_HUMAN | (P05091) | Aldehyde dehydrogenase, mitochondrial precursor (EC 1.2.1.3) (ALDH class 2) (ALDH) |
| SPYA_HUMAN | (P21549) | Serine--pyruvate aminotransferase (EC 2.6.1.51) (SPT) (Alanine--glyoxylate aminotransferase) |
| HBD_HUMAN | (P02042) | Hemoglobin delta subunit (Hemoglobin delta chain) (Delta-globin) |
| THIL_HUMAN | (P24752) | Acetyl-CoA acetyltransferase, mitochondrial precursor (EC 2.3.1.9) |
| LDHA_HUMAN | (P00338) | L-lactate dehydrogenase A chain (EC 1.1.1.27) (LDH-A) (LDH muscle subunit) (LDH-M) |
| ANXA6_HUMAN | (P08133) | Annexin A6 (Annexin VI) (Lipocortin VI) (P68) (P70) (Protein III) (Chromobindin-20) |
| GOGB1_HUMAN | (Q14789) | Golgi autoantigen, golgin subfamily B member 1 (Golgin-245) (Macrogolgin) |
| G3P1_HUMAN | (P00354) | Glyceraldehyde-3-phosphate dehydrogenase, muscle (EC 1.2.1.12) (GAPDH) |
| ANK2_HUMAN | (Q01484) | Ankyrin-2 (Brain ankyrin) (Ankyrin B) (Ankyrin, nonerythroid) |
| THIM_HUMAN | (P42765) | 3-ketoacyl-CoA thiolase, mitochondrial (EC 2.3.1.16) (Beta-ketothiolase) |
| SYNE1_HUMAN | (Q8NF91) | Nesprin-1 (Nuclear envelope spectrin repeat protein 1) (Synaptic nuclear envelope protein 1) (Syne-1) (Myocyte nuclear envelope protein 1) (Myne-1) (Enaptin) |
| F16P1_HUMAN | (P09467) | Fructose-1,6-bisphosphatase 1 (EC 3.1.3.11) (D-fructose-1,6-bisphosphate 1-phosphohydrolas |
| IQGA2_HUMAN | (Q13576) | Ras GTPase-activating-like protein IQGAP2 |
| HBG1_HUMAN | (P69891) | Hemoglobin gamma-1 chain (Hemoglobin gamma-A chain) (Hb F-gamma) |
| MLL3_HUMAN | (Q8NEZ4) | Myeloid/lymphoid or mixed-lineage leukemia protein 3 homolog |
| NEBU_HUMAN | (P20929) | Nebulin |
| ZF106_HUMAN | (Q9H2Y7) | Zinc finger protein 106 homolog (Zfp-106) (Zinc finger protein 474) |
| TENS_HUMAN | (Q9HBL0) | Tensin |
| UGPA1_HUMAN | (Q07131) | UTP--glucose-1-phosphate uridylyltransferase 1 (EC 2.7.7.9) (UDP-glucose pyrophosphorylase |
| ADH7_HUMAN | (P40394) | Alcohol dehydrogenase class IV mu/sigma chain (EC 1.1.1.1) (Retinol dehydrogenase) |
| FXL19_HUMAN | (Q6PC12) | F-box/LRR-repeat protein 19 (F-box and leucine-rich repeat protein 19) |
| ACSL5_HUMAN | (Q9ULC5) | Long-chain-fatty-acid--CoA ligase 5 (EC 6.2.1.3) (Long-chain acyl-CoA synthetase 5) |
| PARL_HUMAN | (Q8TEW8) | Amyotrophic lateral sclerosis 2 chromosome region candidate gene protein 19 |
| THIO_HUMAN | (P10599) | Thioredoxin (ATL-derived factor) (AOF) (Surface associated sulphydryl protein) (SASP) |
| ATPSH_HUMAN | (O75947) | ATP synthase D chain, mitochondrial (EC 3.6.3.14) |
| LYRIC_HUMAN | (Q86UE4) | LYRIC protein (Lysine-rich CEACAM1 co-isolated protein) (3D3/lyric) |
| DHSO_HUMAN | (Q00796) | Sorbitol dehydrogenase (EC 1.1.1.14) (L-iditol 2-dehydrogenase) |
| NCOA6_HUMAN | (Q14686) | Nuclear receptor coactivator 6 (Amplified in breast cancer-3 protein) (Activating signal cointegrator-2) (ASC-2) (Peroxisome proliferator-activated receptor-interacting protein) |
| SPTN5_HUMAN | (Q9NRC8) | Spectrin beta chain, brain 4 (Spectrin, non-erythroid beta chain 4) (Beta-V spectrin) |
| GNRP_HUMAN | (Q13972) | Guanine nucleotide-releasing protein (GNRP) (Ras-specific nucleotide exchange factor CDC25) (Ras-specific guanine nucleotide-releasing factor) |
| CLAP1_HUMAN | (Q7Z460) | CLIP-associating protein 1 (Cytoplasmic linker-associated protein 1) (Multiple asters homolog 1) |
| CJ012_HUMAN | (Q8N6S5) | Protein C10orf12 |
| HYES_HUMAN | (P34913) | Epoxide hydrolase 2 (EC 3.3.2.3) (Soluble epoxide hydrolase) (SEH) (Epoxide hydratase) (Cy |
| M3K3_HUMAN | (Q99759) | Mitogen-activated protein kinase kinase kinase 3 (EC 2.7.1.37) (MAPK/ERK kinase kinase 3) (MEK kinase 3) (MEKK 3) |
| DHX37_HUMAN | (Q8IY37) | Probable ATP-dependent helicase DHX37 (DEAH-box protein 37) |
| TENX_HUMAN | (P22105) | Tenascin-X precursor (TN-X) (Hexabrachion-like protein) |
| DYH5_HUMAN | (Q8TE73) | Ciliary dynein heavy chain 5 (Axonemal beta dynein heavy chain 5) (HL1) |
| APC_HUMAN | (P25054) | Adenomatous polyposis coli protein (APC protein) |
| RTEL1_HUMAN | (Q9NZ71) | Regulator of telomere elongation helicase 1 (Helicase-like protein NHL) |
| LRFN5_HUMAN | (Q96NI6) | Leucine-rich repeat and fibronectin type-III domain containing protein 5 precursor |
| ANR11_HUMAN | (Q6UB99) | Ankyrin repeat domain protein 11 (Ankyrin repeat-containing cofactor 1) |
| MYO1A_HUMAN | (O94832) | Myosin Ia (Brush border myosin I) (BBM-I) (BBM1) (Myosin I heavy chain) (MIHC) |
| PAPOA_HUMAN | (P51003) | Poly(A) polymerase alpha (EC 2.7.7.19) (PAP) (Polynucleotide adenylyltransferase alpha) |
| CF151_HUMAN | (Q61EG0) | U11/U12 snRNP 48 kDa protein |
| CO7A1_HUMAN | (Q02388) | Collagen alpha 1(VII) chain precursor (Long-chain collagen) (LC collagen) |
| MYO5A_HUMAN | (Q9Y4I1) | Myosin-5A (Myosin Va) (Dilute myosin heavy chain, non-muscle) (Myosin heavy chain 12) (Myoxin) |
| CAR10_HUMAN | (Q9BWT7) | Caspase recruitment domain protein 10 (CARD-containing MAGUK protein 3) (Carma 3) |
| ZNF44_HUMAN | (P15621) | Zinc finger protein 44 (Zinc finger protein KOX7) (Gonadotropin inducible transcription repressor-2) |
| ZEP1_HUMAN | (P15822) | Zinc finger protein 40 (Human immunodeficiency virus type I enhancer-binding protein 1) |
| UN13B_HUMAN | (O14795) | Unc-13 homolog B (Munc13-2) (munc13) |
| GBF1_HUMAN | (Q92538) | Golgi-specific brefeldin A-resistance guanine nucleotide exchange factor 1 (BFA-resistant |
| CHD8_HUMAN | (Q9HCK8) | Chromodomain-helicase-DNA-binding protein 8 (CHD-8) (Helicase with SNF2 domain 1) (Fragment) |
| AL1A2_HUMAN | (O94788) | Retinal dehydrogenase 2 (EC 1.2.1.36) (RalDH2) (RALDH 2) (RALDH(II)) |
| ATM_HUMAN | (Q13315) | Serine-protein kinase ATM (EC 2.7.1.37) (Ataxia telangiectasia mutated) (A-T. mutated) |
| PCLO_HUMAN | (Q9Y6V0) | Piccolo protein (Aczonin) |
| CELR3_HUMAN | (Q9NYQ7) | Cadherin EGF LAG seven-pass G-type receptor 3 precursor (Flamingo homolog 1) |
| AKAP2_HUMAN | (O94Y2D5) | A kinase anchor protein 2 (Protein kinase A anchoring protein 2) (PRKA2) (AKAP-2) |
| CO4A3_HUMAN | (O60259) | Collagen alpha 3(IV) chain precursor (Goodpasture antigen) |
| ATBF1_HUMAN | (Q15911) | Alpha-fetoprotein enhancer binding protein (AT motif-binding factor) (AT-binding transcrip |
| ABCAC_HUMAN | (Q86UK0) | ATP-binding cassette sub-family A member 12 (ATP-binding cassette transporter 12) |
| G3PT_HUMAN | (O14556) | Glyceraldehyde-3-phosphate dehydrogenase, testis-specific (EC 1.2.1.12) (Spermatogenic cel |
| RASL1_HUMAN | (O95294) | RasGAP-activating-like protein 1 |
| BRCA2_HUMAN | (P51587) | Breast cancer type 2 susceptibility protein (Fanconi anemia group D1 protein) |
| COPB2_HUMAN | (P35606) | Coatomer beta' subunit (Beta'-coat protein) (Beta'-COP) (p102) |
| HS90B_HUMAN | (P08238) | Heat shock protein HSP 90-beta (HSP 84) (HSP 90) |
| NIPBL_HUMAN | (Q6KC79) | Nipped-B-like protein (Delangin) (SCC2 homolog) |
| ATR_HUMAN | (Q13535) | Serine-protein kinase ATR (EC 2.7.1.37) (Ataxia telangiectasia and Rad3-related protein) |
| DYH9_HUMAN | (Q9NYC9) | Ciliary dynein heavy chain 9 (Axonemal beta dynein heavy chain 9) |
| BPAEA_HUMAN | (Q94833) | Bullous pemphigoid antigen 1, isoforms 6/9/10 (Trabeculin-beta) (Bullous pemphigoid antigen) (BPA) (Hemidesmosomal plaque protein) (Dystonia musculorum protein) (Dystonin) |
| SUPT3_HUMAN | (O75486) | Transcription initiation protein SPT3 homolog (SPT3-like protein) |
| NYX_HUMAN | (Q9GZU5) | Nyctalopin precursor |
| HOOK2_HUMAN | (Q96ED9) | Hook homolog 2 (h-hook2) (hHK2) |
| PLK1_HUMAN | (P53350) | Serine/threonine-protein kinase PLK1 (EC 2.7.1.37) (Polo-like kinase 1) (PLK-1) (Serine/threonine-protein kinase 13) (STPK13) |
| KIF14_HUMAN | (Q15058) | Kinesin-like protein KIF14 |
| TM16E_HUMAN | (Q75V66) | Transmembrane protein 16E (Gnathodiaphyseal dysplasia 1 protein) |
| CAC1B_HUMAN | (Q00975) | Voltage-dependent N-type calcium channel alpha-1B subunit |
| COEA2_HUMAN | (P12110) | Collagen alpha 2(VI) chain precursor |
| POK3_HUMAN | (Q9WJR5) | HERV-K 19q12 provirus ancestral Pol protein (HERV-K(C19) Pol protein) |
| LAMA3_HUMAN | (Q16787) | Laminin alpha-3 chain precursor (Epiligrin 170 kDa subunit) (E170) (Nicein alpha subunit) |
| MPIP1_HUMAN | (P30304) | M-phase inducer phosphatase 1 (EC 3.1.3.48) (Dual specificity phosphatase Cdc25A) |
| DESP_HUMAN | (P15924) | Desmoplakin (DP) (250/210 kDa paraneoplastic pemphigus antigen) |
| ZN490_HUMAN | (Q9ULM2) | Zinc finger protein 490 |
| IF2C4_HUMAN | (Q9HCK5) | Eukaryotic translation initiation factor 2C 4 (eIF2C 4) (eIF-2C 4) (Argonaute-4) |
| DISC1_HUMAN | (Q9NRI5) | Disrupted in schizophrenia 1 protein |
| HS90A_HUMAN | (P07900) | Heat shock protein HSP 90-alpha (HSP 86) |
| LGR8_HUMAN | (Q8WXD0) | Relaxin receptor 2 (Leucine-rich repeat-containing G-protein coupled receptor 8) |
| FBX18_HUMAN | (Q8NFZ0) | F-box only protein 18 (EC 3.6.1.-) (F-box DNA helicase 1) |
| GEM4_HUMAN | (P57678) | Component of gems 4 (Gemin-4) (p97) |
| ARP2_HUMAN | (P61160) | Actin-like protein 2 (Actin-related protein 2) |
| ZSWM5_HUMAN | (Q9P217) | Zinc finger SWIM domain containing protein 5 |
| SMRC2_HUMAN | (Q8TAQ2) | SWI/SNF-related matrix-associated actin-dependent regulator of chromatin subfamily C membe |
| VINC_HUMAN | (P18206) | Vinculin (Metavinculin) |
| SMCA4_HUMAN | (P51532) | Possible global transcription activator SNF2L4 (SNF2-beta) (BRG-1 protein) (Mitotic growth and transcripton activator) (Brahma protein homolog 1) (SWI/SNF related matrix associated actin dependent regulator of chromatin subfamily A |
| BC11A_HUMAN | (Q9H165) | B-cell lymphoma/leukemia 11A (B-cell CLL/lymphoma 11A) (COUP-TF interacting protein 1) |
| FBX46_HUMAN | (Q6PJB1) | (Ecotropic viral integration site 9 protein) (EVI-9) |
| JPH3_HUMAN | (Q8WXH2) | F-box only protein 46 (F-box only protein 34-like) |
| RL10_HUMAN | (P27635) | Junctophilin-3 (Junctophilin type 3) (JP-3) |
| 4ET_HUMAN | (Q9NRA8) | 60S ribosomal protein L10 (QM protein) (Tumor suppressor QM) (Laminin receptor homolog) |
| STK31_HUMAN | (Q9BXU1) | Eukaryotic translation initiation factor 4E transporter (eIF4E transporter) (4E-T) |
| CEP2_HUMAN | (Q9BV73) | Serine/threonine-protein kinase 31 (EC 2.7.1.37) (Serine/threonine-protein kinase NYD-SPK) |
| CN145_HUMAN | (Q6ZU80) | Centrosomal protein 2 (Centrosome and Nek2-associated protein 1) (C-NAP1) (Centrosome protein 250) (Centrosome associated protein CEP250) |
| RP1L1_HUMAN | (Q8WN71) | Protein C14orf145 |
| KIF3C_HUMAN | (O14782) | Retinitis pigmentosa 1-like 1 protein |
| UBP8_HUMAN | (P40818) | Kinesin-like protein KIF3C |
| LAMA2_HUMAN | (P24043) | Ubiquitin carboxyl-terminal hydrolase 8 (EC 3.1.2.15) (Ubiquitin thiolesterase 8) (Ubiquitin-specific processing protease 8) (Deubiquitinating enzyme 8) (hUBPy) |
| SMC3_HUMAN | (Q9UQE7) | Laminin alpha-2 chain precursor (Laminin M chain) (Merosin heavy chain) |
| GOGA3_HUMAN | (Q08378) | Structural maintenance of chromosome 3 (Chondroitin sulfate proteoglycan 6) (Chromosome-associated polypeptide) (hCAP) (Bamacan) (Basement membrane-associated chondroitin |
| ACTZ_HUMAN | (P61163) | Golgi autoantigen, golgin subfamily A member 3 (Golgin-160) (Golgi complex-associated protein of 170 kDa) (GCP170) |
| | | Alpha-centractin (Centractin) (Centrosome-associated actin homolog) (Actin-RPV) (ARP1) |

表２　ラット尿中でMASCOT検索により同定されたタンパク質

| NAME | ID | Description |
|---|---|---|
| ALBU_RAT | (P02770) | Serum albumin precursor |
| MUP_RAT | (P02761) | Major urinary protein precursor (MUP) (Alpha-2u-globulin) (Alpha(2)-euglobulin) |
| EGF_RAT | (P07522) | Pro-epidermal growth factor precursor (EGF) [Contains: Epidermal growth factor] |
| 22P1_RAT | (P22282) | Cystatin-related protein 1 precursor (CRP-1) (Prostatic 22 kDa glycoprotein P22K16/P22K20) |
| UROM_RAT | (P27590) | Uromodulin precursor (Tamm-Horsfall urinary glycoprotein) (THP) |
| CPI3_RAT | (P05544) | Contrapsin-like protease inhibitor 3 precursor (CPI-23) (Serine protease inhibitor 1) (SPI |
| CPI1_RAT | (P05545) | Contrapsin-like protease inhibitor 1 precursor (CPI-21) (Kallikrein-binding protein) (KBP) |
| AMPN_RAT | (P15684) | Aminopeptidase N (EC 3.4.11.2) (rAPN) (Alanyl aminopeptidase) (Microsomal aminopeptidase) |
| AMBP_RAT | (Q64240) | AMBP protein precursor [Contains: Alpha-1-microglobulin; Inter-alpha-trypsin inhibitor lig |
| KLK7_RAT | (P36373) | Glandular kallikrein-7, submandibular/renal precursor (EC 3.4.21.35) (Tissue kallikrein) |
| TRFE_RAT | (P12346) | Serotransferrin precursor (Transferrin) (Siderophilin) (Beta-1-metal binding globulin) |
| A1AT_RAT | (P17475) | Alpha-1-antiproteinase precursor (Alpha-1-antitrypsin) (Alpha-1-proteinase inhibitor) |
| UP1_RAT | (P81827) | Urinary protein 1 precursor (RUP-1) (Liver regeneration-related protein LRRG05) |
| UP3_RAT | (P83121) | Urinary protein 3 precursor (RUP-3) |
| ACTB_RAT | (P60711) | Actin, cytoplasmic 1 (Beta-actin) |
| UP2_RAT | (P81828) | Urinary protein 2 precursor (RUP-2) |
| ACTC_RAT | (P68035) | Actin, alpha cardiac (Alpha-cardiac actin) |
| ACTS_RAT | (P68136) | Actin, alpha skeletal muscle (Alpha-actin-1) |
| AMYP_RAT | (P00689) | Pancreatic alpha-amylase precursor (EC 3.2.1.1) (PA) (1,4-alpha-D-glucan glucanohydrolase) |
| PSC3_RAT | (P02780) | Prostatic steroid-binding protein C3 chain precursor (Prostatein peptide C3) |
| KACA_RAT | (P01836) | Ig kappa chain C region, A allele |
| GGT1_RAT | (P07314) | Gamma-glutamyltranspeptidase 1 precursor (EC 2.3.2.2) (Gamma-glutamyltransferase 1) |
| HEMO_RAT | (P20059) | Hemopexin precursor |
| SODC_RAT | (P07632) | Superoxide dismutase [Cu-Zn] (EC 1.15.1.1) |
| SLC31_RAT | (Q64319) | Neutral and basic amino acid transport protein rBAT (B(0,+)-type amino acid transport prot |
| KLK9_RAT | (P07647) | Submandibular glandular kallikrein-9 precursor (EC 3.4.21.35) (Tissue kallikrein) (S3 kall |
| HBB2_RAT | (P11517) | Hemoglobin beta-2 subunit (Hemoglobin beta-2 chain) (Beta-2-globin) (Hemoglobin beta chain |
| KLK1_RAT | (P00758) | Nerve growth factor gamma chain precursor (EC 3.4.21.35) (Gamma-NGF) (Tissue kallikrein) |
| B2MG_RAT | (P07151) | Beta-2-microglobulin precursor |
| MEP1A_RAT | (Q64230) | Meprin A alpha-subunit precursor (EC 3.4.24.18) (Endopeptidase-2) (MEP-1) (Endopeptidase-2) |
| NOTC2_RAT | (Q9QW30) | Neurogenic locus notch homolog protein 2 precursor (Notch 2) [Contains: Notch 2 extracellu |
| PBAS_RAT | (P15399) | Probasin precursor (PB) (M-40) |
| SYCP1_RAT | (Q03410) | Synaptonemal complex protein 1 (SCP-1 protein) |
| SPA3M_RAT | (Q63556) | Serine protease inhibitor A3M precursor (Serine protease inhibitor 2.4) (SPI-2.4) |
| HBA_RAT | (P01946) | Hemoglobin alpha-1/2 subunit (Hemoglobin alpha-1/2 chain) (Alpha-1/2-globin) |
| ATOX1_RAT | (Q9WUC4) | Copper transport protein ATOX1 (Metal transport protein ATX1) |
| PSC2_RAT | (P02781) | Prostatic steroid-binding protein C2 chain precursor (Prostatein peptide C2) |
| MYH7_RAT | (P02564) | Myosin heavy chain, cardiac muscle beta isoform (MyHC-beta) |
| DNMT1_RAT | (Q9Z330) | DNA (cytosine-5)-methyltransferase 1 (EC 2.1.1.37) (Dnmt1) (DNA methyltransferase I) |
| KLK12_RAT | (P36376) | Glandular kallikrein-12, submandibular/renal precursor (EC 3.4.21.35) (Tissue kallikrein) |
| MYH10_RAT | (Q9JLT0) | Myosin-10 (Myosin heavy chain, nonmuscle IIb) (Nonmuscle myosin heavy chain IIb) |
| PLEC1_RAT | (P30427) | Plectin 1 (PLTN) (PCN) |
| MYH6_RAT | (P02563) | Myosin heavy chain, cardiac muscle alpha isoform (MyHC-alpha) |
| 22P2_RAT | (P22283) | Cystatin-related protein 2 precursor (Prostatic 22 kDa glycoprotein P22K15) |
| PCLO_RAT | (Q9JKS6) | Piccolo protein (Multidomain presynaptic cytomatrix protein) |
| MOES_RAT | (O35763) | Moesin (Membrane-organizing extension spike protein) |
| GRK4_RAT | (P70507) | G protein-coupled receptor kinase 4 (EC 2.7.1.-) (G protein-coupled receptor kinase GRK4) |
| CAC1C_RAT | (P22002) | Voltage-dependent L-type calcium channel alpha-1C subunit (Voltage-gated calcium channel alpha subunit Cav1.2) |
| CAC1H_RAT | (Q9EQ60) | Voltage-dependent T-type calcium channel alpha-1H subunit |
| KLK3_RAT | (P15950) | Glandular kallikrein-3, submandibular (EC 3.4.21.35) (Tissue kallikrein) (S1 kallikrein) |
| XAB2_RAT | (Q99PK0) | XPA-binding protein 2 (Adapter protein ATH-55) |
| PLMN_RAT | (Q01177) | Plasminogen precursor (EC 3.4.21.7) [Contains: Plasmin heavy chain A; Activation peptide; |
| EZRI_RAT | (P31977) | Ezrin (p81) (Cytovillin) (Villin-2) |
| EI2BD_RAT | (Q63186) | Translation initiation factor eIF-2B delta subunit (eIF-2B GDP-GTP exchange factor) |
| PGFRA_RAT | (P20786) | Alpha platelet-derived growth factor receptor precursor (EC 2.7.1.112) (PDGF-R-alpha) |
| FAS_RAT | (P12785) | Fatty acid synthase (EC 2.3.1.85) [Includes: [Acyl-carrier-protein] S-acetyltransferase (E |
| THYG_RAT | (P06882) | Thyroglobulin precursor |
| CO4_RAT | (P08649) | Complement C4 precursor [Contains: Complement C4 beta chain; Complement C4 alpha chain; C4 |
| ARNT_RAT | (P41739) | Aryl hydrocarbon receptor nuclear translocator (ARNT protein) (Dioxin receptor, nuclear translocator) (Hypoxia-inducible factor 1 beta) |
| MAP2_RAT | (P15146) | Microtubule-associated protein 2 (MAP 2) (MAP-2) |
| MYH11_RAT | (Q63862) | Myosin-11 (Myosin heavy chain, smooth muscle isoform) (SMMHC) (Fragments) |
| HD_RAT | (P51111) | Huntingtin (Huntington's disease protein homolog) (HD protein) |
| CSAD_RAT | (Q64611) | Cysteine sulfinic acid decarboxylase (EC 4.1.1.29) (Sulfinoalanine decarboxylase) |
| FOLH1_RAT | (P70627) | Glutamate carboxypeptidase II (EC 3.4.17.21) (Membrane glutamate carboxypeptidase) |
| RIP3_RAT | (Q9ERE6) | Rho-interacting protein 3 (p116RIP) (RIP3) |
| PLD2_RAT | (P70498) | Phospholipase D2 (EC 3.1.4.4) (PLD 2) (Choline phosphatase 2) (Phosphatidylcholine-hydroly |
| MAST1_RAT | (Q810W7) | Microtubule-associated serine/threonine-protein kinase 1 (EC 2.7.1.37) (Syntrophin-associated serine/threonine-protein kinase) |
| DPOG1_RAT | (Q9QYV8) | DNA polymerase gamma subunit 1 (EC 2.7.7.7) (Mitochondrial DNA polymerase catalytic subuni |
| P85A_RAT | (Q63787) | Phosphatidylinositol 3-kinase regulatory alpha subunit (PI3-kinase p85-alpha subunit) (PtdIns-3-kinase p85-alpha) (PI3K) |
| PAK3_RAT | (Q62829) | Serine/threonine-protein kinase PAK 3 (EC 2.7.1.37) (p21-activated kinase 3) (PAK-3) (Beta |
| CLH_RAT | (P11442) | Clathrin heavy chain |
| SHAN3_RAT | (Q9JLU4) | SH3 and multiple ankyrin repeat domains 3 (Shank3) (Proline-rich synapse associated protein 2) (ProSAP2) (SPANK-2) |
| PRIC1_RAT | (Q71QF9) | Prickle-like protein 1 (REST/NRSF-interacting LIM domain protein 1) |
| GBRG2_RAT | (P18508) | Gamma-aminobutyric-acid receptor gamma-2 subunit precursor (GABA(A) receptor) |
| B3A2_RAT | (P23347) | Anion exchange protein 2 (Non-erythroid band 3-like protein) (AE2 anion exchanger) (Solute carrier family 4 member 2) (B3RP) |
| NOTC1_RAT | (Q07008) | Neurogenic locus notch homolog protein 1 precursor (Notch 1) [Contains: Notch 1 extracellu |
| VGFR1_RAT | (P53767) | Vascular endothelial growth factor receptor 1 precursor (EC 2.7.1.112) (VEGFR-1) (Tyrosine-protein kinase receptor FLT) (FLT-1) |
| YME1_RAT | (Q925S8) | ATP-dependent metalloprotease YME1L1 (EC 3.4.24.-) (YME1-like protein 1) (ATP-dependent me |
| CYLN2_RAT | (O55156) | Cytoplasmic linker protein 2 (Cytoplasmic linker protein 115) (CLIP-115) |
| PRS7_RAT | (Q63347) | 26S protease regulatory subunit 7 (MSS1 protein) |
| CAND1_RAT | (P97536) | Cullin-associated NEDD8-dissociated protein 1 (Cullin-associated and neddylation-dissociated protein 1) (p120 CAND1) |
| ABCC9_RAT | (Q63563) | Sulfonylurea receptor 2 |
| MYST3_RAT | (Q5TKR9) | Histone acetyltransferase MYST3 (EC 2.3.1.48) (EC 2.3.1.-) (MYST protein 3) |
| SPTN2_RAT | (Q9QWN8) | Spectrin beta chain, brain 2 (Spectrin, non-erythroid beta chain 2) (Beta-III spectrin) (S |
| ABLM2_RAT | (Q6KC51) | Actin-binding LIM protein 2 (Actin-binding LIM protein family member 2) (abLIM2) |
| CASP1_RAT | (P43527) | Caspase-1 precursor (EC 3.4.22.36) (CASP-1) (Interleukin-1 beta convertase) (IL-1BC) |
| IL6RA_RAT | (P22273) | Interleukin-6 receptor alpha chain precursor (IL-6R-alpha) (IL-6R 1) |
| MINP1_RAT | (O35217) | Multiple inositol polyphosphate phosphatase 1 precursor (EC 3.1.3.62) (Inositol (1,3,4,5)-tetrakiphosphate 3-phosphatase) |
| INP5E_RAT | (Q9WVR1) | 72 kDa inositol polyphosphate 5-phosphatase (EC 3.1.3.36) (Phosphatidylinositol-4,5-bispho |
| DVL1_RAT | (Q9WVB9) | Segment polarity protein dishevelled homolog DVL-1 (Dishevelled-1) (DSH homolog 1) |
| P55G_RAT | (Q63789) | Phosphatidylinositol 3-kinase regulatory gamma subunit (PI3-kinase p85-gamma subunit) (PtdIns-3-kinase p85-gamma) (p55PIK) |
| KCMA1_RAT | (Q62976) | Calcium-activated potassium channel alpha subunit 1 (Calcium-activated potassium channel, |
| TNR1A_RAT | (P22934) | Tumor necrosis factor receptor superfamily member 1A precursor (p60) (TNF-R1) |
| MYO1E_RAT | (Q63356) | Myosin Ie (Myosin heavy chain myr 3) |
| PLCG2_RAT | (P24135) | 1-phosphatidylinositol-4,5-bisphosphate phosphodiesterase gamma 2 (EC 3.1.4.11) |
| PSD1_RAT | (O88761) | 26S proteasome non-ATPase regulatory subunit 1 (26S proteasome regulatory subunit RPN2) |
| ALDOC_RAT | (P09117) | Fructose-bisphosphate aldolase C (EC 4.1.2.13) (Brain-type aldolase) |
| MYH3_RAT | (P12847) | Myosin heavy chain, fast skeletal muscle, embryonic |
| PCSK5_RAT | (P41413) | Proprotein convertase subtilisin/kexin type 5 precursor (EC 3.4.21.-) |
| KCNH1_RAT | (Q63472) | Potassium voltage-gated channel subfamily H member 1 |
| SRP54_RAT | (Q6AYB5) | Signal recognition particle 54 kDa protein (SRP54) |
| PTPRV_RAT | (Q64612) | Receptor-type tyrosine-protein phosphatase V precursor (EC 3.1.3.48) |
| CELR2_RAT | (Q9QYP2) | Cadherin EGF LAG seven-pass G-type receptor 2 (Multiple epidermal growth factor-like domains 3) (Fragment) |
| CAC1A_RAT | (P54282) | Voltage-dependent P/Q-type calcium channel alpha-1A subunit (Voltage-gated calcium channel |
| MBTP1_RAT | (Q9WTZ3) | Membrane-bound transcription factor site-1 protease precursor (EC 3.4.21.-) |
| KCNQ1_RAT | (Q9Z0N7) | Potassium voltage-gated channel subfamily KQT member 1 (Voltage-gated potassium channel subunit Kv7.1) |
| RORB_RAT | (P45446) | Nuclear receptor ROR-beta (Nuclear receptor RZR-beta) |
| SULF1_RAT | (Q8VI60) | Extracellular sulfatase Sulf-1 precursor (EC 3.1.6.-) (Sulfatase FP) (RSulfFP1) |
| MBB1A_RAT | (O35821) | Myb-binding protein 1A (PAR-interacting protein) (PIP) |

表３　アセトン沈殿の有無により同定されたタンパク質の比較

| アセトン沈殿より同定されたタンパク質 | | 直接消化により同定されたタンパク質 | |
|---|---|---|---|
| **22P1_RAT** | **MUP_RAT** | **22P1_RAT** | LRRC7_RAT |
| **A1AT_RAT** | MYH11_RAT | **A1AT_RAT** | MAP2_RAT |
| **ADA10_RAT** | MYO5A_RAT | **ADA10_RAT** | **MEP1A_RAT** |
| | MYST3_RAT | AGT2_RAT | MPDZ_RAT |
| | **MYT1L_RAT** | AK1A1_RAT | **MUP_RAT** |
| **ALBU_RAT** | **NOTC2_RAT** | **ALBU_RAT** | MYH3_RAT |
| AMBP_RAT | PADI2_RAT | ARBK2_RAT | MYO9B_RAT |
| AMPN_RAT | PBAS_RAT | **ATOX1_RAT** | MYST2_RAT |
| APBB1_RAT | **PCLO_RAT** | ATP5H_RAT | **MYT1L_RAT** |
| ARAF_RAT | **PCSK5_RAT** | B2MG_RAT | **NOTC1_RAT** |
| AT2B2_RAT | | BAT2_RAT | NOTC2_RAT |
| AT2B3_RAT | | BRCA2_RAT | PAHX_RAT |
| **ATOX1_RAT** | | CABIN_RAT | PARG_RAT |
| BSN_RAT | PER2_RAT | CASP1_RAT | **PCLO_RAT** |
| CAN1_RAT | PGFRA_RAT | CD166_RAT | **PCSK5_RAT** |
| CAPON_RAT | PLCB2_RAT | CELR2_RAT | PDZK3_RAT |
| CG031_RAT | PLD1_RAT | CELR3_RAT | **PLEC1_RAT** |
| **CH60_RAT** | **PLEC1_RAT** | **CH60_RAT** | PLK2_RAT |
| CPI1_RAT | PSC2_RAT | CLAP2_RAT | PRIC1_RAT |
| CPI3_RAT | **PSC3_RAT** | CO4_RAT | **PSC3_RAT** |
| CSEN_RAT | RNZ2_RAT | COA1_RAT | RBM30_RAT |
| CYLN2_RAT | ROCK1_RAT | COF1_RAT | RIMS1_RAT |
| **DNMT1_RAT** | RP3A_RAT | CPI3_RAT | RIP3_RAT |
| EDNRB_RAT | SC10A_RAT | **DNMT1_RAT** | RPA1_RAT |
| EGF_RAT | SCN9A_RAT | EF2K_RAT | SHAN3_RAT |
| EPHA7_RAT | SGTA_RAT | GGT1_RAT | SIA10_RAT |
| GSK3A_RAT | SLC31_RAT | GRP75_RAT | **SODC_RAT** |
| HBB2_RAT | SMC1A_RAT | HBA_RAT | SYCP1_RAT |
| HD_RAT | **SODC_RAT** | HD_RAT | TCPD_RAT |
| HEMO_RAT | SPA3M_RAT | HXK3_RAT | TFAM_RAT |
| HS90B_RAT | SPTN2_RAT | IDH3A_RAT | TGM4_RAT |
| ITB4_RAT | TM55B_RAT | INHBA_RAT | THB2_RAT |
| ITSN1_RAT | TRFE_RAT | ITPR3_RAT | TRIM3_RAT |
| JMJ1A_RAT | UN13C_RAT | K6PP_RAT | UHRF1_RAT |
| KACA_RAT | **UP1_RAT** | KGP2_RAT | **UP1_RAT** |
| KCNH1_RAT | **UP2_RAT** | **KLK1_RAT** | **UP2_RAT** |
| **KLK1_RAT** | **UP3_RAT** | **KLK7_RAT** | **UP3_RAT** |
| **KLK7_RAT** | **UROM_RAT** | KLK9_RAT | **UROM_RAT** |
| LAMB2_RAT | XAB2_RAT | LIPA3_RAT | VLCS_RAT |
| **MEP1A_RAT** | YMEL1_RAT | LRP4_RAT | |

太字は22種の共通タンパク

表４　既知標準混合サンプルの ICAT 法による定量予測

| | | | | | | | | | | |
|---|---|---|---|---|---|---|---|---|---|---|
| **BSA** | | | | | | | | | | |
| Time | m/z-Light | m/z-Heavy | 価数 | 親イオン[M+H] | Area-Light | Area-Heavy | H : L | Ave. | 理論比 | 実測/理論 |
| 22. 055-22. 297 | 684. 3770 | 687. 3873 | 3 | 2051. 1150 | 1892 | 1421 | 0. 751 | | | |
| 16. 134-16. 376 | 807. 4157 | 811. 9334 | 2 | 1613. 8234 | 1589 | 1486 | 0. 936 | 0. 843 | 1. 0 | 0. 843 |
| **LDH-M** | | | | | | | | | | |
| 16. 617-17. 222 | 709. 8737 | 714. 3826 | 2 | 1418. 7394 | 13497 | 7673 | 0. 569 | | 0. 667 | 0. 853 |
| **SOD** | | | | | | | | | | |
| 20. 122-20. 363 | 586. 3432 | 590. 8665 | 2 | 1171. 6784 | 30469 | 20652 | 0. 678 | | | |
| 21. 451-22. 297 | 766. 1079 | 769. 1191 | 3 | 2296. 3077 | 3570 | 1691 | 0. 474 | 0. 576 | 0. 5 | 1. 152 |
| **RNase A** | | | | | | | | | | |
| 14. 322-14. 926 | 543. 2754 | 547. 7853 | 2 | 1085. 5428 | 5303 | 6704 | 1. 264 | | | |
| 24. 109-24. 832 | 798. 7677 | 801. 7729 | 3 | 2394. 2871 | 12550 | 18428 | 1. 468 | | | |
| 14. 322-14. 926 | 837. 9311 | 842. 4474 | 2 | 1674. 8542 | 5699 | 8335 | 1. 463 | | | |
| 24. 349-24. 712 | 1197. 6519 | 1202. 1606 | 2 | 2394. 2958 | 19162 | 27464 | 1. 433 | 1. 407 | 1. 5 | 0. 938 |

表５　cICAT 法による個別サイトゾルタンパク量の比較（プールドサイトゾルに対し）

| HG23 (40 /41) | | HK27 (49 /54) | | HG30 (53 /56) | | HG43 (55 /56) | | （比決定/同定） |
|---|---|---|---|---|---|---|---|---|
| Accession # | Ratio | Accession # | Ratio | Accession # | Ratio | Accession # | Avg H:L | |
| | | AATM_HUMAN (P00505) | 0.8684 | AATM_HUMAN (P00505) | 0.9525 | | | |
| ADH4_HUMAN (P08319) | 1.2111 | ADH4_HUMAN (P08319) | 0.934 | ADH4_HUMAN (P08319) | 1.0718 | ADH4_HUMAN (P08319) | 0.5559 | |
| ADHA_HUMAN (P07327) | 1.3931 | ADHA_HUMAN (P07327) | 1.1474 | ADHA_HUMAN (P07327) | 1.2279 | ADHA_HUMAN (P07327) | 1.4886 | |
| ADHB_HUMAN (P00325) | 1.4522 | ADHB_HUMAN (P00325) | 1.1494 | ADHB_HUMAN (P00325) | 1.2739 | ADHB_HUMAN (P00325) | 1.5482 | |
| ADHG_HUMAN (P00326) | 1.4426 | ADHG_HUMAN (P00326) | 1.1585 | ADHG_HUMAN (P00326) | 1.2348 | ADHG_HUMAN (P00326) | 1.5434 | |
| | | | | ADHX_HUMAN (P11766) | | | | |
| | | | | ADO_HUMAN (Q06278) | 0.9646 | ADO_HUMAN (Q06278) | 1.0638 | |
| AKC1_HUMAN (Q04828) | 1.1886 | AKC1_HUMAN (Q04828) | 1.4352 | AKC1_HUMAN (Q04828) | 1.2054 | AKC1_HUMAN (Q04828) | 1.4061 | |
| AKC2_HUMAN (P52895) | 1.1886 | AKC2_HUMAN (P52895) | 1.4352 | AKC2_HUMAN (P52895) | 1.2054 | AKC2_HUMAN (P52895) | 1.4061 | |
| | | | | AKC4_HUMAN (P17516) | 1.0883 | AKC4_HUMAN (P17516) | 1.0101 | |
| ALBU_HUMAN (P02768) | 1.8222 | ALBU_HUMAN (P02768) | 2.5498 | ALBU_HUMAN (P02768) | 1.2229 | ALBU_HUMAN (P02768) | 2.4161 | |
| ALFB_HUMAN (P05062) | 1.303 | ALFB_HUMAN (P05062) | 1.6318 | ALFB_HUMAN (P05062) | 1.5547 | ALFB_HUMAN (P05062) | 1.054 | |
| | | | | AMPL_HUMAN (P28838) | 1.0188 | | | |
| ARGI_HUMAN (P05089) | 0.7392 | ARGI_HUMAN (P05089) | 0.9815 | ARGI_HUMAN (P05089) | | ARGI_HUMAN (P05089) | 0.9039 | |
| | | ASSY_HUMAN (P00966) | 1.1922 | ASSY_HUMAN (P00966) | 1.4727 | ASSY_HUMAN (P00966) | 1.1136 | |
| BHMT_HUMAN (Q93088) | 1.0255 | BHMT_HUMAN (Q93088) | 0.9035 | BHMT_HUMAN (Q93088) | 1.134 | BHMT_HUMAN (Q93088) | 0.9016 | |
| | | BUP1_HUMAN (Q9UBR1) | 1.2446 | | | | | |
| | | | | CATA_HUMAN (P04040) | 1.5469 | CATA_HUMAN (P04040) | 1.2424 | |
| | | | | CH60_HUMAN (P10809) | 0.8029 | | | |
| | | | | | | CATB_HUMAN (P07858) | 1.2609 | |
| CPSM_HUMAN (P31327) | 1.1447 | CPSM_HUMAN (P31327) | 1.2454 | CPSM_HUMAN (P31327) | 1.2469 | CPSM_HUMAN (P31327) | 1.4751 | |
| | | DEF1_HUMAN (P59665) | 0.8348 | | | | | |
| DHA1_HUMAN (P00352) | 1.0551 | DHA1_HUMAN (P00352) | 1.2413 | DHA1_HUMAN (P00352) | 1.1567 | DHA1_HUMAN (P00352) | 1.1799 | |
| DHAM_HUMAN (P05091) | 1.1082 | DHAM_HUMAN (P05091) | 1.0569 | DHAM_HUMAN (P05091) | 1.5259 | DHAM_HUMAN (P05091) | 1.3544 | |
| DHCA_HUMAN (P16152) | 1.0551 | DHCA_HUMAN (P16152) | 1.1767 | DHCA_HUMAN (P16152) | 1.3265 | DHCA_HUMAN (P16152) | 1.2183 | |
| DHE3_HUMAN (P00367) | 1.5682 | | | | | DHE3_HUMAN (P00367) | 1.2133 | |
| DHSO_HUMAN (Q00796) | 1.5494 | | | | | | | |
| DOPD_HUMAN (P30046) | 0.5875 | DOPD_HUMAN (P30046) | 1.0614 | DOPD_HUMAN (P30046) | 0.7498 | | | |
| | | | | | | DHE4_HUMAN (P49448) | 1.1604 | |
| | | | | ECH1_HUMAN (Q13011) | 1.0437 | | | |
| | | | | ECHM_HUMAN (P30084) | 1.4051 | ECHM_HUMAN (P30084) | 1.0101 | |
| ENOA_HUMAN (P06733) | 1.101 | | | ENOA_HUMAN (P06733) | 1.2876 | ENOA_HUMAN (P06733) | 1.4443 | |
| ENOB_HUMAN (P13929) | 1.0362 | | | ENOB_HUMAN (P13929) | 1.1582 | | | |
| ENOG_HUMAN (P09104) | 1.0362 | | | ENOG_HUMAN (P09104) | 1.1582 | | | |
| | | | | F16P_HUMAN (P09467) | 1.1654 | F16P_HUMAN (P09467) | 0.8796 | |
| FAAA_HUMAN (P16930) | 0.9861 | FAAA_HUMAN (P16930) | 0.9671 | FAAA_HUMAN (P16930) | 1.199 | | | |
| FAS_HUMAN (P49327) | 1.3834 | FAS_HUMAN (P49327) | 2.3302 | FAS_HUMAN (P49327) | 2.7567 | | | |
| FTCD_HUMAN (Q95954) | 1.3394 | FTCD_HUMAN (Q95954) | 1.4488 | | | FTCD_HUMAN (Q95954) | 0.9726 | |
| G3P1_HUMAN (P00354) | 1.1018 | G3P1_HUMAN (P00354) | 1.2617 | G3P1_HUMAN (P00354) | 1.3352 | G3P1_HUMAN (P00354) | 1.1307 | |
| G3P2_HUMAN (P04406) | 1.0108 | G3P2_HUMAN (P04406) | 1.1408 | G3P2_HUMAN (P04406) | 1.2569 | G3P2_HUMAN (P04406) | 1.011 | |
| | | | | GABT_HUMAN (P80404) | | | | |
| GHPR_HUMAN (Q9UBQ7) | 1.2733 | GHPR_HUMAN (Q9UBQ7) | 1.4692 | GHPR_HUMAN (Q9UBQ7) | 1.3409 | GHPR_HUMAN (Q9UBQ7) | 1.5782 | |
| | | | | | | GLMT_HUMAN (Q14749) | 1.8924 | |
| | | | | | | GLRX_HUMAN (P35754) | 0.8096 | |
| GLYC_HUMAN (P34896) | 0.9373 | GLYC_HUMAN (P34896) | 0.7653 | GLYC_HUMAN (P34896) | 1.0333 | GLYC_HUMAN (P34896) | 1.1558 | |
| GTT1_HUMAN (P30711) | | | | GTT1_HUMAN (P30711) | | GTT1_HUMAN (P30711) | 1.4208 | |
| | | HAO1_HUMAN (Q9UJM8) | | | | HAO1_HUMAN (Q9UJM8) | 1.6067 | |
| HBB_HUMAN (P02023) | 2.1978 | HBB_HUMAN (P02023) | 3.4439 | HBB_HUMAN (P02023) | 1.8415 | HBB_HUMAN (P02023) | 1.611 | |
| | | HBD_HUMAN (P02042) | | HBD_HUMAN (P02042) | 2.0921 | | | |
| | | | | HEM2_HUMAN (P13716) | 1.2531 | | | |
| | | HMCM_HUMAN (P54868) | 1.3687 | | | HMCM_HUMAN (P54868) | 1.0913 | |
| HNT1_HUMAN (P49773) | 0.7414 | | | | | | | |
| | | | | HS71_HUMAN (P08107) | 2.1376 | HS71_HUMAN (P08107) | 1.5178 | |
| | | | | HS76_HUMAN (P17066) | 2.1376 | HS76_HUMAN (P17066) | 1.5178 | |
| | | | | | | IDHC_HUMAN (O75874) | 1.0817 | |
| IF41_HUMAN (P60842) | 1.1561 | | | | | IF41_HUMAN (P60842) | 1.5259 | |
| IF42_HUMAN (Q14240) | 1.1561 | | | | | IF42_HUMAN (Q14240) | 1.5259 | |
| | | KAC_HUMAN (P01834) | 3.2598 | | | KAC_HUMAN (P01834) | 1.4945 | |
| LDHA_HUMAN (P00338) | 0.9771 | LDHA_HUMAN (P00338) | 0.7848 | LDHA_HUMAN (P00338) | 1.2233 | LDHA_HUMAN (P00338) | 1.197 | |
| LDHB_HUMAN (P07195) | 0.9771 | LDHB_HUMAN (P07195) | 0.8138 | LDHB_HUMAN (P07195) | 1.0166 | LDHB_HUMAN (P07195) | 1.0767 | |
| LDHC_HUMAN (P07864) | 0.9771 | LDHC_HUMAN (P07864) | 0.8138 | LDHC_HUMAN (P07864) | 1.0166 | LDHC_HUMAN (P07864) | 1.0767 | |
| | | LGUL_HUMAN (Q04760) | 1.0446 | | | LGUL_HUMAN (Q04760) | 0.993 | |
| | | MDHM_HUMAN (P40926) | 0.9712 | | | | | |
| | | | | METL_HUMAN (Q00266) | 1.7116 | | | |
| | | MIF_HUMAN (P14174) | 1.26 | MIF_HUMAN (P14174) | 1.1918 | MIF_HUMAN (P14174) | 0.8533 | |
| | | | | MPB1_HUMAN (P22712) | 1.4313 | MPB1_HUMAN (P22712) | 1.5787 | |

□ いずれにおいてもH：L比が出ているタンパク質
HG30以外においてH：L比が出ているタンパク質
■ HG30以外で同定されているタンパク質

厚生労働科学研究費補助金（萌芽的先端医療技術推進研究事業）
分担研究報告書

# 細胞レベルでのメタボロミクス技術の開発

分担研究者：小原　有弘　(独)医薬基盤研究所　細胞資源研究室研究員

研究要旨

薬剤による毒性の予測を行うためのシステムを構築するため、尿試料ならびに細胞試料を用いたNMRによるメタボノミクス技術の開発を目的とした。本年度はマウス病態モデルから採取した尿試料のNMR解析を行い、薬剤による毒性マーカーと病態時のマーカーとの相互比較に利用できるマーカー検索を実施し、病態特異的なマーカー検出を行った。

## A. 研究目的

ヒトに投与して初めて起こる副作用を予測するため網羅的な遺伝子発現解析が注目されトキシコゲノミクスと呼ばれる研究が実施されてきた。しかし毒性の予測までには至っていないのが現状である。本研究では非侵襲試料を用いたメタボノミクス解析手法を確立し、トキシコゲノミクスで得られた網羅的な遺伝子発現情報を補完し、毒性予測につながる評価系開発を行うことを目的としている。そこで我々はよりスクリーニング研究に適していると考えられる培養細胞を用いたメタボノミクス解析技術の確立を目指す。本年度は予備検討として医薬基盤研究所・実験動物開発室で保有している疾患モデルマウスの尿を用いてNMR解析を行い、感度の評価並び解析手法の選択を行った。今後技術開発により、細胞レベルでのメタボロミクス研究を推進する。ヒト肝・腎細胞およびヒト由来培養細胞を用いて、毒性を有する薬剤の網羅的遺伝子発現

## B. 研究方法

＜疾患モデルマウスに関して＞

EL マウス

ヒト自然発症てんかん発作モデルマウスであり、体位変換刺激などにより容易にてんかん発作を引き起こす。

ICGN/M ネフローゼマウス

加齢とともに腎炎を発症し、腎原発性（一次）ネフローゼを示す。ヒトネフローゼモデルとして利用される。病態の進行に伴ってすなわち腎糸球体基底膜の肥厚、糸球体足突起の消失やメサンギウム細胞の増殖をともなわないメサンギウム領域の拡張などを呈するようになる。さらに病態末期においては尿細管拡張、尿細管間質部病変も認められるようになる。また病態の進行にともない、タンパク尿、低タンパク血症、高脂血症および腎性貧血の症状も認められる。これまでの病理組織学的所見や臨床生化学的検査結果から、これまでになかったヒト

における特発性腎炎症候群の有用な実験モデルと考えられる。

GM1 ガングリオシドーシスモデルマウス
(β-galactosidase knockout mouse, BKO)

GM1 ガングリオシドーシスは、リソゾーム性 β-ガラクトシダーゼ (β-Gal) 遺伝子の変異に基づく神経遺伝病であり、代表的なリソゾーム性蓄積症の一つである。本症は致死的で、難病に指定されており、有効な治療法はない。

4 C30

シアル酸転移酵素を導入したトランスジェニックマウス。ホモ導入個体は 7 ヶ月程度で心拡大を伴う呼吸不全で全例死亡する（野口ら、2003)。心臓の症状から、このマウスは拡張型心筋症モデルマウスとなっている。

C57BL/6J *bg*

C57BL/6J を遺伝的背景にもつベージュマウス。 ♂は *bg*/*bg*、♀は *bg*/+で維持されている。ナチュラルキラー細胞および細胞依存性細胞障害活性を示すキラー細胞の活性が低く、Chediak-Higashi 病のモデルとして用いることができる。

＜NMR 測定に関して＞

ブルカーバイオスピン社の協力を得て、UltraShield Plus 500MHz NMR により $^{1}$H-NMR を測定した。

## C. 結果

本分担研究では、細胞レベルでのメタボロミクス技術の開発を目的としており、NMR を用いた高感度解析技術を採用する予定である。しかし、導入予定である 800MHzNMR 設備整備が遅れており、NMR 解析はブルカーバイオスピン社にご協力頂き実施した。本年度は細胞レベルでのメタボノミクス解析の前段階として、従来用いられている尿試料を用いた解析を行った。医薬基盤研究所・実験動物開発室で保有する疾患モデルマウス 5 系統ならびにそれらの野生型であるマウス 3 系統、モルモットの尿試料を用いて NMR での病態時における解析を実施した。今回用いた疾患モデルマウスは EL マウス（てんかんモデル),ICGN/M マウス(ネフローゼモデル), GM1 マウス（リソゾーム病モデル), 4C30 マウス（心筋症モデル), C57BL/6J *bg* （Chediak-Higashi 病モデル）である。NMR 解析の結果を図 1 に示した。

スペクトルを見ると違いが鮮明であり、特にモルモットとマウスの種の違い、ICGN/M マウス（ネフローゼモデル）の違いは明らかであった。モルモットのスペクトラムは 8ppm 付近のシグナル、3.5ppm 付近のシグナルなど特徴的なものと、マウスとシグナルは同じであるが積分値が異なるものという特徴を示し、これらは種の違い特に食餌の違いが大きく影響している結果であると考えられる。また、ICGN/M マウスにおいては 1～1.5ppm 付近に特徴的なブロードピークが見られ、これはネフローゼという病態に特徴的なタンパク尿を反映しているシグナルであると考えられる。その他のマウスに関してもシグナルの詳細解析を実施しており、病態特異的と考えられるシグナルを認めている。また、今回の測定に用いたサンプルを用いて PCA（主成分分析）を行った

(図２)。PCA による解析では 4C30 マウス（心筋症モデル），C57BL/6J *bg* (Chediak-Higashi 病モデル)，モルモットが成分１、成分２を用いて他のマウスと非常によく分離できた。本解析ではモルモットを含めた全てのサンプルを用いたが、病態モデルマウスを非常によく分離解析できている。

## D. 考察・結論

細胞レベルでのメタボロミクス技術の開発を目的として、高感度かつ簡便解析が実施できる NMR を採用することとした。医薬基盤研究所では本年度 800MHz 高感度 NMR を設備整備する予定であったが、その整備が遅れている。本年度はブルカーバイオスピン社の協力を得て、NMR 解析を実施し、細胞レベルでの解析前段階として病態モデルマウスの尿試料を用いた。今回の解析結果から、実験動物を用いることによって病態時の毒性マーカーを見出すことは比較的容易であり、今後の更なる解析によって新たな毒性マーカーを見出すことができると思われる。しかし、実験動物は非常に厳密に制御された環境下で維持・管理されている動物であり、薬剤投与による毒性などの検出には非常に有用であると考えられるが、ヒト試料を考えた場合、生活環境・飲食物・体質など様々な要因によってスペクトラム変化が起こり、解析を困難にすることが容易に予測できる。今回用いたモルモットにおいても、食餌の違いを主とする主の違いが明らかであり、尿を試料とした場合には、それらをどのようにして克服するかが今後の課題となる。また、細胞レベルでのメタボノミクス解析においては、NMR が非常に高感度であり、前処理を必要としないことから、細胞を薬剤処理し、一定時間後超音波破砕した細胞試料をそのまま解析あるいは除タンパク処理後解析する方法を検討しており、実際に NMR 解析したところ、ノイズ等を気にすることなく解析が可能であるという結果を得ている。今後は毒性のある薬剤を選択し、その毒性のタイプを詳細解析できる手法の確立を目指す。

## E.健康危険情報

なし

## F. 学会発表

小原有弘，水澤博・国内培養細胞研究資源の現状と JCRB 細胞バンクにおける品質管理・日本組織培養学会（2005.5.26）

Arihiro Kohara, Tohru Masui, Hiroshi Mizusawa・Training Procedures in Cell Culture・Society for In Vitro Biology (2005.6.6)

Arihiro Kohara, Yutaka Ozawa, Setusko Shioda, Tohru Masui, Masao Takeuchi, Hiroshi Mizusawa・Developing an In Vitro Gene Expression Assay for Predicting Hepatotoxicity.・9th ICEM Satellite Meeting on Txicogenomics（2005.9.1）

小原有弘・ナショナルバイオリソースプロジェクト（NBRP）の研究成果発表展示・日本分子生物学会（2005.12.7-9）

論文

Yamada K, Suzuki T, Kohara A, Kato TA, Hayashi M, Mizutani T, Saeki K.・Nitrogen-substitution effect on in vivo mutagenicity of chrysene.・ Mutat Res. 2005 586(1):1-17

## G. 知的財産権の出願・登録状況

登録および登録予定共になし

図1

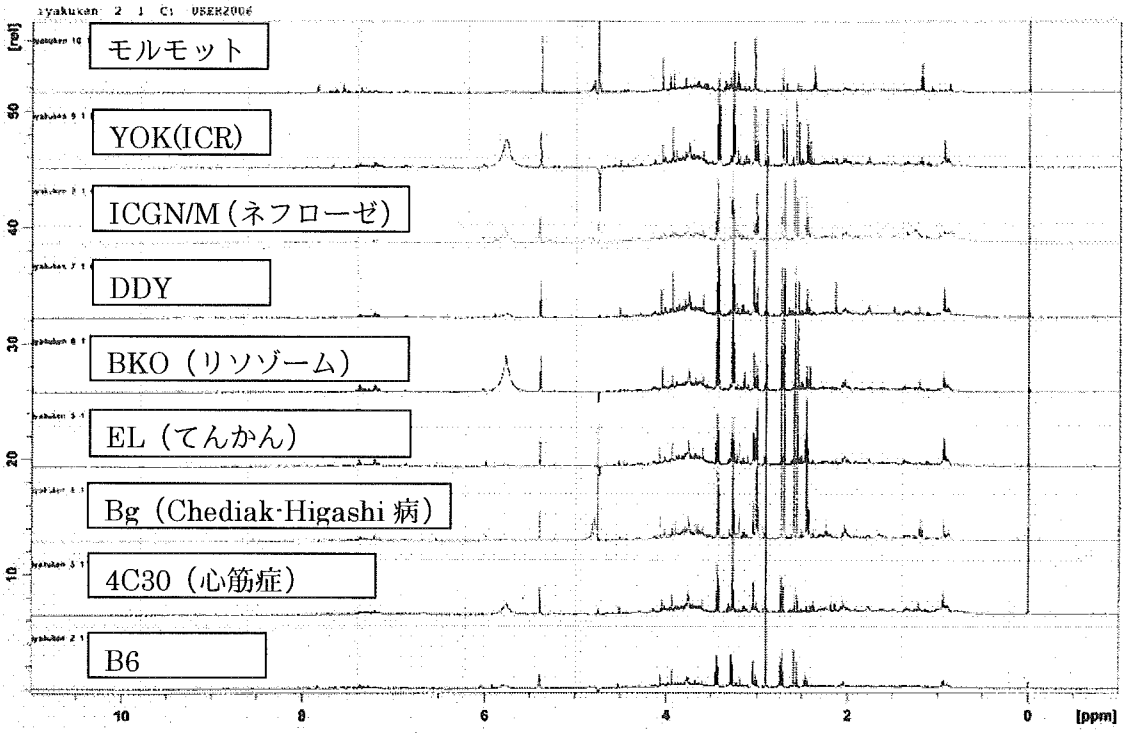
モルモット
YOK(ICR)
ICGN/M（ネフローゼ）
DDY
BKO（リソゾーム）
EL（てんかん）
Bg（Chediak-Higashi 病）
4C30（心筋症）
B6
10
8
6
4
2
0
[ppm]

図2

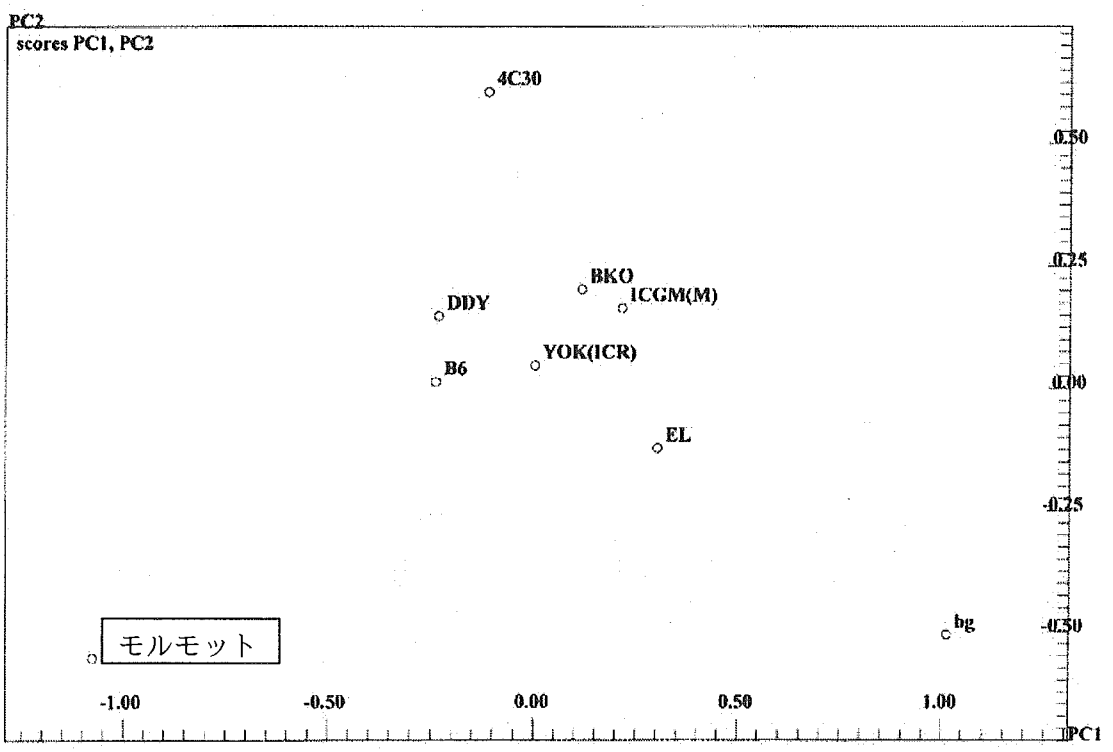
PC2
scores PC1, PC2
4C30
BKO
ICGM(M)
DDY
YOK(ICR)
B6
EL
bg
モルモット
0.50
0.25
0.00
-0.25
-0.50
-1.00
-0.50
0.00
0.50
1.00
PC1

# 研究成果の刊行に関する一覧表

雑誌

| 発表者氏名 | 論文タイトル名 | 発表誌名 | 巻号 | ページ | 出版年 |
|---|---|---|---|---|---|
| I. Nakanishi, C. Nishizawa, K. Ohkubo, K. Takeshita, K. Suzuki, T. Ozawa, S. M. Hecht, M. Tanno, S. Sueyoshi, N. Miyata, H. Okuda, S. Fukuzumi, N. Ikota, K. Fukuhara | Hydroxyl Radical Generation via Photoreduction of a Simple Pyridine *N*-Oxide by an NADH Analogue | *Org. Biomol. Chem* | **3** | 3263 – 3265 | 2005 |
| I. Nakanishi, T. Kawashima, K. Ohkubo, H. Kanazawa, K. Inami, M. Mochizuki, K. Fukuhara, H. Okuda, T. Ozawa, S. Itoh, S. Fukuzumi, and N. Ikota | Electron-Tansfer Mechanism in Radical-Scavenging Reactions by a Vitamin E Model in a Protic Medium | *Org. Biomol. Chem* | **3** | 626 – 629 | 2005 |
| Takayoshi Suzuki, Osamu Nagae, Yuka Kato, Hidehiko Nakagawa, Kiyoshi Fukuhara, Naoki Miyata, | Photo-induced Nitric Oxide Release from Nitrobenzene Derivatives | *J. Am. Chem. Soc* | **127 (33)** | 11720-11726 | 2005 |
| Takayoshi Suzuki, Azusa Matsuura, Akiyasu Kouketsu, Sinya Hisakawa, Hidehiko Nakagawa, Naoki Miyata | Design and synthesis of non-hydroxamate histone deacetylase inhibitors; identification of a selective histone acetylating agent | *Bioorganic & Medicinal Chemistry* | **13** | 4332-4342 | 2005 |
| Takayoshi Suzuki, Yuki Nagano, Akiyasu Kouketsu, Azusa Matsuura, Sakiko Maruyama, Mineko Kurotaki, Hidehiko Nakagawa, Naoki Miyata | Novel inhibitors of human histone deacetylases: design, synthesis, enzyme inhibition, and cancer cell growth inhibition of SAHA-based non-hydroxamates | *J. Med. Chem.* | **48(4)** | 1019-1032 | 2005 |
| Uhinya Usui, Takayoshi Suzuki, Yoshifumi Hattori, Kazuma Etoh, Hiroki Fujieda, Makoto Nishizuka, Masayoshi Imagawa, Hidehiko Nakagawa, Kohfuku Kohda, Naoki Miyata | Design, synthesis and biological activity of novel PPARg ligands based on rosiglitazone and 15d-PGJ2 | *Bioorganic & Medicinal Chemistry Letters* | **15** | 1547-1551 | 2005 |
| Takayoshi Suzuki, Azusa Matsuura, Akiyoshi Kouketsu, Hidehiko Nakagawa, Naoki Miyata, | Identification of a potent non-hydroxamate histone deacetylase inhibitor by mechanism- based drug design | *Bioorganic & Medicinal Chemistry Letters* | **15** | 331-335 | 2005 |
| Takayoshi Suzuki, Hidehiko Nakagawa, Naoki Miyata | Molecularly tageted approch to cancer therapy: design, synthesis and biological activity of non-hydroxamate histone deacetylase inhibitors | *J. of Syn. Org. Chem* | **63(10)** | 1004-1015 | 2005 |
| T. Suzuki, N. Miyata | Non-hydroxamate Histone Deacetylase Inhibitors | *Curr. Med. Chem* | **12** | 2867-2880 | 2005 |

| | | | | | |
|---|---|---|---|---|---|
| Yamada K, Suzuki T, Kohara A, Kato TA, Hayashi M, Mizutani T, Saeki K. | Nitrogen-substitution effect on in vivo mutagenicity of chrysene | Mutat Res. | 586 | 1-17 | 2005 |
| Kanayasu-Toyoda T, Fujino T, Oshizawa T, Suzuki T, Nishimaki-Mogami T, Sato Y, Sawada J, Inoue K, Shudo K, Ohno Y, Yamaguchi T | HX531, a retinoid X receptor antagonist, inhibited the 9-cis retinoic acid-induced binding with steroid receptor coactivator-1 as detected by surface plasmon resonance | J Steroid Biochem Mol Biol | 94 | 303-309 | 2005 |
| Kawakami T, Hoshida Y, Kanai F, Tanaka Y, Tateishi K, Ikenoue T, Obi S, Sato S, Teratani T, Shiina S, Kawabe T, Suzuki T, Hatano N, Taniguchi H, Omata M. | Proteomic analysis of sera from hepatocellular carcinoma patients after radiofrequency ablation treatment | Proteomics | 16 | 4287-4295 | 2005 |
| K. Fukuhara, M. Nagakawa, I. Nakanishi, K. Ohkubo, K. Imai, S. Urano, S. Fukuzumi, T. Ozawa, N. Ikota, M. Mochizuki, N. Miyata, H. Okuda | Structural Basis for DNA Cleaving-Activity of Resveratrol om the Presence of Cu(II) | *Bioorg. Med. Chem* | **14** | 1437-1443 | 2006 |
| T. Suzuki, N. Miyata | Rational Design of Non-hydroxamate Histone Deacetylase Inhibitors | *Mini Rev. Med. Chem* | **5** | in press | 2006 |
| T. Suzuki and N. Miyata | Epigenetic Control Using Natural Products and Synthetic Molecules | *Curr. Med. Chem* | **13** | in press | 2006 |
| Shinya Usui, Hiroki Fujieda, Takayoshi Suzuki, Naoaki Yoshida, Hidehiko Nakagawa and Naoki Miyata | Identification of novel PPARγ ligands by the structural modification of a PPARγ ligand | *Bioorganic & Medicinal Chemistry Letters* | **16** | in press | 2006 |

COMMUNICATION

OBC
www.rsc.org/obc

# Hydroxyl radical generation *via* photoreduction of a simple pyridine *N*-oxide by an NADH analogue†

**Ikuo Nakanishi,*[a,b] Chiho Nishizawa,[a,c] Kei Ohkubo,[b] Keizo Takeshita,[d] Kazuo T. Suzuki,[c] Toshihiko Ozawa,[a] Sidney M. Hecht,[e] Masayuki Tanno,[f] Shoko Sueyoshi,[f] Naoki Miyata,[g] Haruhiro Okuda,[f] Shunichi Fukuzumi,[b] Nobuo Ikota*[a] and Kiyoshi Fukuhara*[f]**

[a] *Redox Regulation Research Group, Research Center for Radiation Safety, National Institute of Radiological Sciences (NIRS), Inage-ku, Chiba, 263-8555, Japan. E-mail: nakanis@nirs.go.jp; Fax: +81 43 255 6819; Tel: +81 43 206 3131*

[b] *Department of Material and Life Science, Graduate School of Engineering, Osaka University, SORST, Japan Science and Technology Agency (JST), Suita, Osaka, 565-0871, Japan. E-mail: fukuzumi@chem.eng.osaka-u.ac.jp; Fax: +81 6 6879 7370; Tel: +81 6 6879 7368*

[c] *Department of Toxicology and Environmental Health, Graduate School of Pharmaceutical Science, Chiba University, Chuo-ku, Chiba, 260-8675, Japan*

[d] *Faculty of Pharmaceutical Sciences, Sojo University, Ikeda, Kumamoto, 860-0082, Japan*

[e] *Department of Chemistry and Biology, University of Virginia, Charlottesville, Virginia, 29901, USA*

[f] *Division of Organic Chemistry, National Institute of Health Sciences (NIHS), Setagaya-ku, Tokyo, 158-8501, Japan. E-mail: fukuhara@nihs.go.jp; Fax: +81 3 3707 6950; Tel: +81 3 3700 1141*

[g] *Graduate School of Pharmaceutical Sciences, Nagoya City University, Mizuho-ku, Nagoya, Aichi, 467-8603, Japan*

***Received 5th July 2005, Accepted 22nd July 2005***
***First published as an Advance Article on the web 2nd August 2005***

**Photoreduction of pyridine *N*-oxide, which has a key structure of antitumor agents for hypoxic solid tumors, by 1-benzyl-1,4-dihydronicotinamide in deaerated aprotic media resulted in generation of hydroxyl radical, leading to the oxidation of salicylic acid to 2,3- and 2,5-dihydroxybenzoic acids, and catechol.**

Recently, considerable effort has been made to develop effective drugs against solid tumors, which exist under hypoxic (oxygen-poor) conditions in inefficient vascular systems.[1,2] Tirapazamine (3-amino-1,2,4-benzotriazine 1,4-di-*N*-oxide), which has a heterocyclic *N*-oxide structure, is a clinically promising antitumor agent against hypoxic cells.[3] The DNA damage induced by tirapazamine is proposed to result from the generation of hydroxyl radical (•OH) or the direct oxidation of the deoxyribose backbone of DNA after one-electron reduction of the *N*-oxide to form an activated intermediate.[4–6] However, the actual DNA-damaging species has yet to be clarified. On the other hand, photosensitizers available for photodynamic therapy are advantageous to localize the toxicity to a selected site (tumor cells), thus avoiding toxicity to normal cells.[7] However, since most photosensitizers require $O_2$ to produce reactive oxygen species, they are not effective toward anaerobic solid tumors. Thus, photoactivated compounds, which generate reactive oxygen species under anaerobic conditions, are certainly required for the development of drugs effective against solid tumors without affecting normal cells.

We report herein •OH generation from a simple unsubstituted pyridine *N*-oxide (PyO), which has a largely negative reduction potential, *via* one-electron reduction by photoexcited 1-benzyl-1,4-dihydronicotinamide (BNAH) used as a model compound of dihydronicotinamide adenine dinucleotide (NADH) in DMF under anaerobic conditions. The effects of the substituent at the C-4 position of pyridine *N*-oxides on the mechanism of photoinduced electron transfer from BNAH to pyridine *N*-oxides as well as the reactivity of the corresponding radical anions are clarified based on the spectral and electrochemical data together with the calculated molecular structures by the density functional method, providing a valuable insight into the development of antitumor agents for hypoxic cells.

Salicylic acid (SA) was employed to detect •OH generated in the photoreaction of pyridine *N*-oxides with BNAH in deaerated DMF. SA reacts with •OH to form 2,3-dihydroxybenzoic acid (2,3-DHBA) and 2,5-dihydroxybenzoic acid (2,5-DHBA) as major products and catechol as a minor product.[8–13] These oxidized products of SA are stable and are readily isolated and quantified by a reverse-phase HPLC equipped with an electrochemical detector (HPLC-ECD). SA does not react with $O_2^{\bullet-}$ at an appreciable rate as compared to •OH. Although SA also reacts with singlet oxygen ($^1O_2$), only 2,5-DHBA is formed exclusively, instead of the mixture of 2,3-DHBA, 2,5-DHBA, and catechol.[14]

Aprotic solvents, such as DMF and acetonitrile (MeCN) were used because of the poor solubility of pyridine *N*-oxides toward water, although the reactivity in aqueous media is important for an *in vivo* situation. When a deaerated DMF solution of PyO ($5.0 \times 10^{-3}$ mol dm$^{-3}$) and BNAH ($5.0 \times 10^{-3}$ mol dm$^{-3}$) was irradiated with UV light ($\lambda > 290$ nm) in the presence of SA ($3.2 \times 10^{-2}$ mol dm$^{-3}$), 2,3-DHBA, 2,5-DHBA, and catechol were detected by the HPLC-EC analysis as shown in Fig. 1a. The ratio of the yields of 2,5-DHBA, 2,3-DHBA, and catechol are 48:35:16. Irradiation of PyO or BNAH alone in the presence of SA resulted in no formation of oxidized products of SA (Fig. 1c and d). Under dark conditions, neither DHBA product nor catechol was formed even in the presence of all the components, *i.e.*, PyO, BNAH, and SA (Fig. 1e). These results demonstrate that •OH is generated in the photoreaction of PyO with BNAH in deaerated DMF as shown in Scheme 1. In fact, addition of

† Electronic supplementary information (ESI) available: Transient absorption spectra of the photoreaction between BNAH and PyO (S1), EPR spectrum of $NO_2PyO^{\bullet-}$ (S2), spectral change in the photoreaction between BNAH and $NO_2PyO$ (S3), and DFT minimized structures (S4). See http://dx.doi.org/10.1039/b509447j

DOI:10.1039/b509447j

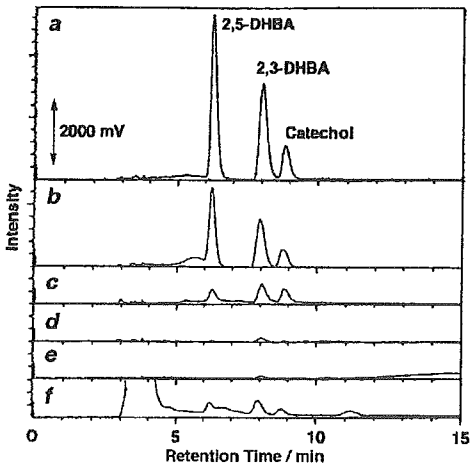


**Fig. 1** HPLC-ECD chromatograms of products formed during irradiation (1 h) of (a) PyO ($5.0 \times 10^{-3}$ mol dm$^{-3}$), BNAH ($5.0 \times 10^{-3}$ mol dm$^{-3}$), and SA ($3.2 \times 10^{-2}$ mol dm$^{-3}$); (b) PyO ($5.0 \times 10^{-3}$ mol dm$^{-3}$), BNAH ($5.0 \times 10^{-3}$ mol dm$^{-3}$), SA ($3.2 \times 10^{-2}$ mol dm$^{-3}$), and ethanol ($5.7 \times 10^{-1}$ mol dm$^{-3}$); (c) PyO ($5.0 \times 10^{-3}$ mol dm$^{-3}$) and SA ($3.2 \times 10^{-2}$ mol dm$^{-3}$); (d) BNAH ($5.0 \times 10^{-3}$ mol dm$^{-3}$) and SA ($3.2 \times 10^{-2}$ mol dm$^{-3}$); (e) PyO ($5.0 \times 10^{-3}$ mol dm$^{-3}$), BNAH ($5.0 \times 10^{-3}$ mol dm$^{-3}$), and SA ($3.2 \times 10^{-2}$ mol dm$^{-3}$) without irradiation; (f) $NO_2PyO$ ($5.0 \times 10^{-3}$ mol dm$^{-3}$), BNAH ($5.0 \times 10^{-3}$ mol dm$^{-3}$), and SA ($3.2 \times 10^{-2}$ mol dm$^{-3}$) in deaerated DMF at 298 K.

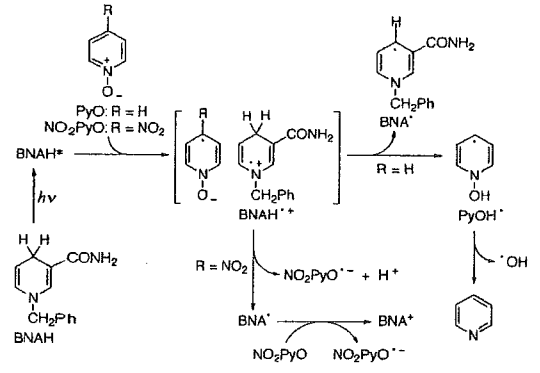


**Scheme 1**

ethanol, which is a •OH scavenger, resulted in a decrease in the yield of three oxidized SA products (Fig. 1b).

Photoirradiation of BNAH is known to give the singlet excited state, BNAH*.[15] The fluorescence of BNAH* is quenched efficiently by the addition of PyO in deaerated MeCN. The quenching rate constant is determined as $1.4 \times 10^{10}$ mol$^{-1}$ dm$^3$ s$^{-1}$, which is close to the diffusion limited value in MeCN. Nanosecond laser excitation of a deaerated MeCN solution of PyO and BNAH results in the formation of PyO$^{\bullet-}$ ($\lambda_{max}$ = 540 nm) and BNAH$^{\bullet+}$ ($\lambda_{max}$ = 380 nm)[16] (see Electronic Supplementary Information, Fig. S1†).

The reaction mechanism of electron-transfer reduction of PyO by BNAH is shown in Scheme 1. Photoinduced electron transfer from BNAH* to PyO takes place to produce a radical ion pair of BNAH$^{\bullet+}$ and PyO$^{\bullet-}$, since the oxidation potential of BNAH* ($E^0_{ox}$ = − 2.65 V *vs.* SCE) determined in DMF[17] is more negative than the reported reduction potential of PyO ($E^0_{red}$ = − 2.30 V) in DMF.[18] Proton transfer from BNAH$^{\bullet+}$, thus produced, to PyO$^{\bullet-}$ gives PyOH• and BNA•. The resulting PyOH• then undergoes the N–O bond cleavage to produce •OH and pyridine. Judging from the more positive oxidation potential of BNA• ($E^0_{ox}$ = − 1.05 V)[17] in DMF than the reduction potential of PyO ($E^0_{red}$ = − 2.30 V),[18] no electron transfer from BNA• to PyO would occur and instead a coupling between two molecules of BNA• may occur to give a dimer $(BNA)_2$.

When PyO is replaced by 4-nitropyridine *N*-oxide ($NO_2PyO$), neither DHBA products nor catechol was produced after irradiation of a deaerated DMF solution containing $NO_2PyO$, BNAH, and SA (Fig. 1f).

This result demonstrates that the radical anion of $NO_2PyO$ ($NO_2PyO^{\bullet-}$) generated in photoinduced electron transfer from BNAH to $NO_2PyO$ is relatively stable and does not undergo the N–O bond cleavage. In fact, an EPR spectrum of $NO_2PyO^{\bullet-}$, which has a *g* value of 2.0054, was observed after irradiation of a deaerated MeCN solution of $NO_2PyO$ and BNAH (Fig. S2a†). The hyperfine coupling constants (hfc) of the observed EPR spectrum of $NO_2PyO^{\bullet-}$ were determined by comparison of the observed spectrum with the computer-simulated spectrum (Fig. S2b†) and they were assigned based on the reported hfc values for $NO_2PyO^{\bullet-}$ in DMF (Fig. S2†).[18]

The UV-vis spectral titration (Fig. S3†) indicates that BNAH acts as a two-electron donor to reduce 2 equiv. of $NO_2PyO$ to $NO_2PyO^{\bullet-}$. Since the $E^0_{ox}$ value of BNAH* (−2.65 V) is more negative than the $E^0_{red}$ value of $NO_2PyO$ (−0.77 V),[18] photoinduced electron transfer from BNAH* to $NO_2PyO$ occurs to give a radical ion pair of $NO_2PyO^{\bullet-}$ and BNAH$^{\bullet+}$. BNAH$^{\bullet+}$ undergoes deprotonation to give BNA•. The delocalization of an electron on the $NO_2PyO^{\bullet-}$ molecule due to the electron-withdrawing $NO_2$ group may preclude the protonation of $NO_2PyO^{\bullet-}$. In fact, no hyperfine structure due to the N–OH proton was observed in the EPR spectrum of $NO_2PyO^{\bullet-}$. The subsequent electron transfer from BNA• to $NO_2PyO$ may also occur rapidly, judging from the $E^0_{ox}$ value of BNA• (−1.05 V), which is lower than the $E^0_{red}$ value of $NO_2PyO$ (−0.77 V).[18] Thus, once photoinduced electron transfer from BNAH to $NO_2PyO$ occurs, 2 equiv of $NO_2PyO^{\bullet-}$ are produced.

DFT calculations using B3LYP/6-31G* basis set for PyOH• and $NO_2PyOH$• were carried out to investigate the difference in the reactivity of radical species of pyridine *N*-oxides depending on a substituent at the C-4 position (Fig. S4†). The calculated N–O bond length in PyOH• (1.50 Å) is significantly longer than that in $NO_2PyOH$• (1.40 Å). This suggests that the N–O bond cleavage in PyOH• may occur much easier than that in $NO_2PyOH$•. Furthermore, PyOH• is significantly bent as indicated by the out-of-plane N–O bond bending angle (*a*) of 152°, whereas $NO_2PyOH$• is relatively flat (*a* = 169°). Similar results have been reported for the N–O bond fragmentation in *N*-methoxy-substituted aromatic compounds.[19] The N–O bond cleavage requires mixing of π* and σ* orbitals, which is achieved by bending the N–O bond out of the plane of the aromatic ring.

In conclusion, photoreduction of a simple pyridine *N*-oxide by BNAH in deaerated aprotic medium resulted in generation of •OH, which can oxidize SA to 2,3-DHBA, 2,5-DHBA, and catechol. The electron-withdrawing group such as $NO_2$ on the aromatic ring can significantly stabilize the radical anion of pyridine *N*-oxide, precluding the subsequent •OH release. We are currently investigating the detailed effects of various substituents on the photoreactivities of pyridine *N*-oxides in the presence of various reducing agents.

## Acknowledgements

This work was partially supported by Grant-in-Aids for Scientific Research (A) (No. 16205020) and for Young Scientist (B) (No. 17790044) from the Ministry of Education, Culture, Sports, Science and Technology, Japan and by the Budget for Nuclear Research of the Ministry of Education, Culture, Sports, Science and Technology, Japan based on the screening and counselling Atomic Energy Commission.

## Notes and references

1 J. M. Brown, *Cancer Res.*, 1999, **59**, 5863.
2 S. Kizaka-Kondoh, M. Inoue, H. Harada and M. Hiraoka, *Cancer Sci.*, 2003, **94**, 1021.

3 D. R. Gandara, P. N. Lara, Z. Goldberg, Q. T. Le, P. C. Mack, D. H. M. Lau and P. H. Gumerlock, *Semin. Oncol.*, 2002, **29**, 102.
4 S. S. Shinde, R. F. Anderson, M. P. Hay, S. A. Gamage and W. A. Denny, *J. Am. Chem. Soc.*, 2004, **126**, 7865.
5 M. Birincioglu, P. Jaruga, G. Chowdhury, H. Rodriguez, M. Dizdaroglu and K. S. Gates, *J. Am. Chem. Soc.*, 2003, **125**, 11607.
6 F. Ban, J. W. Gauld and R. J. Boyd, *J. Am. Chem. Soc.*, 2001, **123**, 7320.
7 B. Armitage, *Chem. Rev.*, 1998, **98**, 1171.
8 R. A. Floyd, J. J. Watson and P. K. Wong, *J. Biochem. Biophys. Methods*, 1984, **10**, 221.
9 R. A. Floyd, R. Henderson, J. J. Watson and P. K. Wong, *Free Radical Biol. Med.*, 1986, **2**, 13.
10 K. O. Hiller and R. L. Wilson, *Biochem. Pharmacol.*, 1983, **32**, 2109.
11 M. Grootveld and B. Halliwell, *Biochem. J.*, 1986, **237**, 499.
12 Z. Maskos, J. D. Rush and W. H. Koppenol, *Free Radical Biol. Med.*, 1990, **8**, 153.
13 B. Kalyanaraman, S. Ramanujam, R. J. Singh, J. Joseph and J. B. Feix, *J. Am. Chem. Soc.*, 1993, **115**, 4007.
14 J. B. Feix and B. Kalyanaraman, *Arch. Biochem. Biophys.*, 1991, **291**, 43.
15 S. Fukuzumi, S. Koumitsu, K. Hironaka and T. Tanaka, *J. Am. Chem. Soc.*, 1987, **109**, 305.
16 (*a*) S. Fukuzumi, O. Inada and T. Suenobu, *J. Am. Chem. Soc.*, 2002, **124**, 14538; (*b*) S. Fukuzumi, O. Inada and T. Suenobu, *J. Am. Chem. Soc.*, 2003, **125**, 4808.
17 The one-electron oxidation potential ($E^0_{ox}$) of BNAH* in DMF was determined as −2.65 V by subtracting the zero–zero transition energy of $\Delta E_{0,0}$ (=3.20 eV) from the $E^0_{ox}$ value of BNAH (0.55 V) in DMF. The $E^0_{ox}$ values of BNAH and BNA$^{\cdot}$ were determined by the second-harmonic alternating current voltammetry (SHACV) technique in deaerated DMF containing 0.1 mol dm$^{-3}$ $Bu_4NClO_4$ as a supporting electrolyte. See: A. M. Bond and D. E. Smith, *Anal. Chem.*, 1974, **46**, 1946.
18 T. Kubota, K. Nishikida, H. Miyazaki, K. Iwatani and Y. Oishi, *J. Am. Chem. Soc.*, 1968, **90**, 5080.
19 (*a*) E. D. Lorance, W. H. Kramer and I. R. Gould, *J. Am. Chem. Soc.*, 2004, **126**, 14071; (*b*) E. D. Lorance, W. H. Kramer and I. R. Gould, *J. Am. Chem. Soc.*, 2002, **124**, 15225.

ARTICLE

OBC www.rsc.org/obc

# Electron-transfer mechanism in radical-scavenging reactions by a vitamin E model in a protic medium

**Ikuo Nakanishi,*[a,b] Tomonori Kawashima,[a,c] Kei Ohkubo,[b] Hideko Kanazawa,[c] Keiko Inami,[d] Masataka Mochizuki,[d] Kiyoshi Fukuhara,[e] Haruhiro Okuda,[e] Toshihiko Ozawa,[a] Shinobu Itoh,[f] Shunichi Fukuzumi*[b] and Nobuo Ikota*[a]**

[a] *Redox Regulation Research Group, Research Center for Radiation Safety, National Institute of Radiological Sciences, Inage-ku, Chiba, 263-8555, Japan. E-mail: nakanis@nirs.go.jp; Fax: +81-43-255-6819; Tel: +81-43-206-3131*

[b] *Department of Material and Life Science, Graduate School of Engineering, Osaka University, SORST, Japan Science and Technology Agency (JST), Suita, Osaka, 565-0871, Japan*

[c] *Department of Physical Pharmaceutical Chemistry, Kyoritsu University of Pharmacy, Minato-ku, Tokyo, 105-8512, Japan*

[d] *Division of Organic and Bioorganic Chemistry, Kyoritsu University of Pharmacy, Minato-ku, Tokyo, 105-8512, Japan*

[e] *Division of Organic Chemistry, National Institute of Health Sciences, Setagaya-ku, Tokyo, 158-8501, Japan*

[f] *Department of Chemistry, Graduate School of Science, Osaka City University, Sumiyoshi-ku, Osaka, 558-8585, Japan*

***Received 11th November 2004, Accepted 29th November 2004***
***First published as an Advance Article on the web 11th January 2005***

The scavenging reaction of 2,2-diphenyl-1-picrylhydrazyl radical (DPPH$^{\bullet}$) or galvinoxyl radical (GO$^{\bullet}$) by a vitamin E model, 2,2,5,7,8-pentamethylchroman-6-ol (**1H**), was significantly accelerated by the presence of $Mg(ClO_4)_2$ in de-aerated methanol (MeOH). Such an acceleration indicates that the radical-scavenging reaction of **1H** in MeOH proceeds *via* an electron transfer from **1H** to the radical, followed by a proton transfer, rather than the one-step hydrogen atom transfer which has been observed in acetonitrile (MeCN). A significant negative shift of the one-electron oxidation potential of **1H** in MeOH (0.63 V *vs.* SCE), due to strong solvation as compared to that in MeCN (0.97 V *vs.* SCE), may result in change of the radical-scavenging mechanisms between protic and aprotic media.

## Introduction

Recently, much attention has been paid to the mechanisms of radical-scavenging reactions of phenolic antioxidants, such as vitamin E (α-tocopherol) and flavonoids, with regard to the development of chemopreventive agents against oxidative stress and associated diseases. There are two mechanisms for the radical-scavenging reactions of phenolic antioxidants: a one-step hydrogen atom transfer from the phenolic OH group; and an electron transfer followed by a proton transfer.[1-3] Metal ions are a powerful tool that can be used to distinguish between these two mechanisms, since electron-transfer reactions are known to be significantly accelerated by their presence.[4] In fact, we have recently reported that scavenging reactions of the galvinoxyl radical (GO$^{\bullet}$) and the cumylperoxyl radical by (+)-catechin in aprotic media, such as acetonitrile (MeCN) and propionitrile, proceed *via* an electron transfer from (+)-catechin to the radicals (which is significantly accelerated by the presence of metal ions, such as $Mg^{2+}$ and $Sc^{3+}$) followed by a proton transfer.[5,6] On the other hand, no effect of $Mg^{2+}$ on the hydrogen-transfer rate from a vitamin E model, 2,2,5,7,8-pentamethylchroman-6-ol (**1H**), to 2,2-bis(4-*tert*-octylphenyl)-1-picrylhydrazyl radical (DOPPH$^{\bullet}$) or GO$^{\bullet}$ in de-aerated MeCN has been observed, indicating that the radical-scavenging reactions of **1H** in MeCN proceed *via* a one-step hydrogen atom transfer rather than *via* electron transfer.[7,8] However, the effects of solvents on the mechanism of radical-scavenging reactions of phenolic antioxidants have yet to be clarified. Leopoldini *et al.* have reported that the bond dissociation enthalpies for O–H bonds and the adiabatic ionization potentials for phenolic antioxidants, calculated with use of density functional theory, do not follow the same trends in gas, water and benzene.[2] Thus, it is of considerable importance to investigate the effects of metal ions on radical-scavenging reactions in various solvents with different polarity.[9]

We report herein that the scavenging reactions of 2,2-diphenyl-1-picrylhydrazyl radical (DPPH$^{\bullet}$) or GO$^{\bullet}$ by the vitamin E model **1H** in de-aerated methanol (MeOH) proceed *via* an electron transfer mechanism rather than *via* a one-step hydrogen atom transfer, which has been observed in de-aerated MeCN. Effects of bases on the radical-scavenging rates were also examined, to clarify whether the actual electron donor is **1H** or the corresponding phenolate anion $\mathbf{1}^-$ in MeOH. Different mechanisms in protic and aprotic solvents are discussed based on kinetic, electrochemical, and EPR data obtained in this study, providing valuable and fundamental information about the radical-scavenging mechanism of phenolic antioxidants.

## Experimental

### Materials

2,2,5,7,8-Pentamethylchroman-6-ol (**1H**) was purchased from Wako Pure Chemical Ind. Ltd., Japan. 2,2-Diphenyl-1-picrylhydrazyl radical (DPPH$^{\bullet}$) and galvinoxyl radical (GO$^{\bullet}$) were commercially obtained from Aldrich. Tetra-*n*-butylammonium perchlorate ($Bu_4NClO_4$), used as a supporting electrolyte for the electrochemical measurements, was purchased from Tokyo Chemical Industry Co., Ltd., Japan, recrystallized from ethanol, and dried under vacuum at 313 K. $Mg(ClO_4)_2$ and methanol (MeOH; spectral grade) were purchased from Nacalai Tesque, Inc., Japan and used as received. Pyridine and 2,6-lutidine were commercially obtained from Wako Pure Chemical Ind. Ltd., Japan and purified by the standard procedure.[10]

DOI: 10.1039/b416572a

### Spectral and kinetic measurements

Since the phenoxyl radical of **1H** (**1**$^{\bullet}$) generated in the reaction of **1H** with radicals readily reacts with molecular oxygen ($O_2$), reactions were carried out under strictly de-aerated conditions. A continuous flow of Ar gas was bubbled through a MeOH solution (3.0 mL) containing DPPH$^{\bullet}$ ($4.8 \times 10^{-5}$ M) and $Mg(ClO_4)_2$ (0–0.3 M) in a square quartz cuvette (10 mm id) with a glass tube neck for 10 min. Air was prevented from leaking into neck of the cuvette with a rubber septum. Typically, an aliquot of **1H** ($2.0 \times 10^{-2}$ M), which was also in de-aerated MeOH, was added to the cuvette with a microsyringe. This led to a reaction of **1H** with DPPH$^{\bullet}$. UV-vis spectral changes associated with the reaction were monitored using an Agilent 8453 photodiode array spectrophotometer. The rates of the DPPH$^{\bullet}$-scavenging reactions of **1H** were determined by monitoring the absorbance change at 516 nm due to DPPH$^{\bullet}$ ($\varepsilon = 1.13 \times 10^4$ M$^{-1}$ cm$^{-1}$) using a stopped-flow technique on a UNISOKU RSP-1000-02NM spectrophotometer. The pseudo-first-order rate constants ($k_{obs}$) were determined by a least-squares curve fit using an Apple Macintosh personal computer. The first-order plots of $\ln(A - A_{\infty})$ *vs.* time ($A$ and $A_{\infty}$ are denoted as the absorbance at the reaction time and the final absorbance, respectively) were linear until three or more half-lives with the correlation coefficient $\rho > 0.999$. The reaction of **1H** with GO$^{\bullet}$ was carried out in the same manner and the rates were determined from the absorbance change at 428 nm due to GO$^{\bullet}$ ($\varepsilon = 1.32 \times 10^5$ M$^{-1}$ cm$^{-1}$). The rate constants of the reactions in the presence of base (pyridine or 2,6-lutidine) were determined in the same manner.

### Electrochemical measurements

The cyclic voltammetry (CV) and second-harmonic alternating current voltammetry (SHACV)[11–16] measurements were performed on an ALS-630A electrochemical analyzer in de-aerated MeOH containing 0.10 M $Bu_4NClO_4$ as a supporting electrolyte. The Pt working electrode (BAS) was polished with BAS polishing alumina suspension and rinsed with acetone before use. The counter electrode was a platinum wire. The measured potentials were recorded with respect to an $Ag/AgNO_3$ (0.01 M) reference electrode. The $E_{1/2}$ values (*vs.* $Ag/AgNO_3$) were converted to those *vs.* SCE by adding 0.29 V.[17] All electrochemical measurements were carried out at 298 K under 1 atm Ar.

### EPR measurements

Typically, an aliquot of a stock solution of **1H** ($2.0 \times 10^{-2}$ M) in de-aerated MeOH was added to the EPR sample tube (0.8 mm id) containing a de-aerated MeOH solution of DPPH$^{\bullet}$ ($2.0 \times 10^{-4}$ M) with a microsyringe under 1 atm Ar. EPR spectra of the phenoxyl radical **1**$^{\bullet}$ produced in the reaction between **1H** and DPPH$^{\bullet}$ were taken on a JEOL X-band spectrometer (JES-RE1XE). The EPR spectra were recorded under non-saturating microwave power conditions. The magnitude of modulation was chosen to optimize the resolution and the signal-to-noise ratio of the observed spectra. The $g$ values and the hyperfine splitting constants were calibrated with a $Mn^{2+}$ marker. Computer simulation of the EPR spectra was carried out using Calleo ESR Version 1.2 program (Calleo Scientific Publisher) on an Apple Macintosh personal computer.

## Results and discussion

### Radical-scavenging reactions of the vitamin E model in de-aerated MeOH

Upon addition of **1H** to a de-aerated MeOH solution of DPPH$^{\bullet}$, the absorption band at 516 nm due to DPPH$^{\bullet}$ disappeared immediately, accompanied by an appearance of the absorption band at 427 nm. Since the absorption band at 427 nm is diagnostic of the phenoxyl radical derived from **1H** (**1**$^{\bullet}$) in MeOH,[18] this spectral change indicates that hydrogen transfer from the phenolic OH group of **1H** to DPPH$^{\bullet}$ takes place to produce **1**$^{\bullet}$ (eqn. (1)). The absorption band of **1**$^{\bullet}$ was shifted from 423 nm in MeCN to 427 nm in MeOH.[7,8] Such a shift in the absorption band of **1**$^{\bullet}$ may be due to a stronger solvation of **1**$^{\bullet}$ in MeOH than in MeCN.

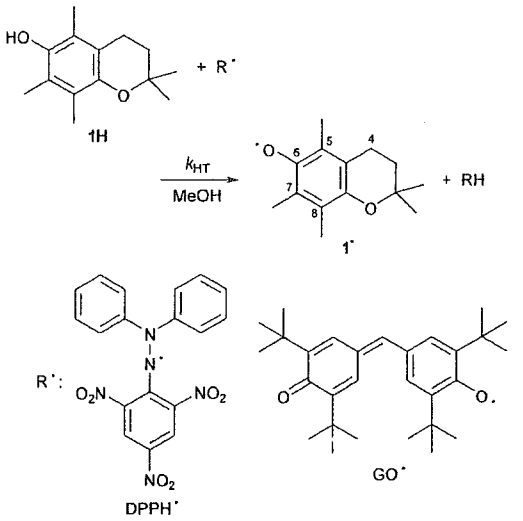


(1)

The rate of the DPPH$^{\bullet}$-scavenging reaction of **1H** was measured by monitoring the decrease in absorbance at 516 nm due to DPPH$^{\bullet}$ using a stopped-flow technique. The decay of the absorbance at 516 nm due to DPPH$^{\bullet}$ obeyed pseudo-first-order kinetics when the concentration of **1H** ([**1H**]) was maintained at more than a 10-fold excess of the DPPH$^{\bullet}$ concentration. The pseudo-first-order rate constants ($k_{obs}$) increase with increasing [**1H**], exhibiting first-order dependence on [**1H**]. From the slope of the linear plot of $k_{obs}$ *vs.* [**1H**], the second-order rate constant ($k_{HT}$) was determined for the radical-scavenging reaction as $1.07 \times 10^3$ M$^{-1}$ s$^{-1}$, in de-aerated MeOH at 298 K. The $k_{HT}$ value thus obtained in de-aerated MeOH is significantly larger than that determined in de-aerated MeCN ($4.35 \times 10^2$ M$^{-1}$ s$^{-1}$).[7] A similar result has been reported by Litwinienko and Ingold.[19] Intermolecularly hydrogen-bonded phenolic OH groups of hydrogen-bond accepting solvents, such as alcohols, are known to be essentially unreactive against radicals.[19] Thus, the enhanced $k_{HT}$ value in MeOH suggested that the reaction mechanism in MeOH may be different from that in MeCN. The GO$^{\bullet}$-scavenging rate constant by **1H** in de-aerated MeOH has also been determined in a same manner by monitoring the decrease in absorbance at 428 nm due to GO$^{\bullet}$ as $2.54 \times 10^3$ M$^{-1}$ s$^{-1}$, which is slightly smaller than that in de-aerated MeCN ($3.32 \times 10^3$ M$^{-1}$ s$^{-1}$).

### Effect of magnesium ion on the rates of radical scavenging reactions

If the radical-scavenging reactions of **1H** involve an electron-transfer process as the rate-determining step, the rates of radical scavenging would be accelerated by the presence of metal ions.[5,6] This was investigated by examining the effect of $Mg(ClO_4)_2$ on the radical-scavenging rates by **1H** in de-aerated MeOH. When $Mg(ClO_4)_2$ is added to the **1H**–DPPH$^{\bullet}$ system in de-aerated MeOH, the rate of DPPH$^{\bullet}$-scavenging reaction by **1H** was significantly accelerated. Such an acceleration was not observed for the DPPH$^{\bullet}$-scavenging reaction by **1H** in MeCN.[7] The $k_{HT}$ value increases linearly with increasing $Mg^{2+}$ concentration ([$Mg^{2+}$]) as shown in Fig. 1a. A similar acceleration effect of $Mg^{2+}$ has been observed for the GO$^{\bullet}$-scavenging reaction by **1H** in de-aerated MeOH (Fig. 1b). Thus, the radical-scavenging reactions in de-aerated MeOH may proceed *via* an electron transfer from **1H** to DPPH$^{\bullet}$ or GO$^{\bullet}$, which is accelerated by the presence of $Mg^{2+}$, followed by proton transfer from **1H**$^{\bullet+}$ to DPPH$^{-}$ or GO$^{-}$ as shown in Scheme 1. In such a case,

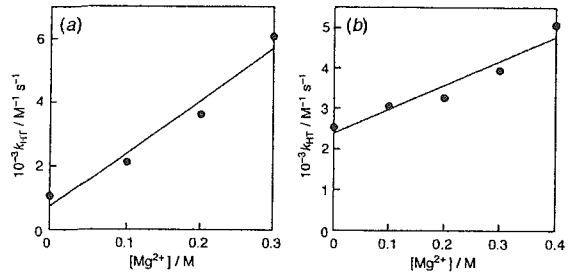


**Fig. 1** Plots of $k_{HT}$ *vs.* [$Mg^{2+}$] in the reaction of **1H** with (a) DPPH$^{\cdot}$ and (b) GO$^{\cdot}$ in de-aerated MeOH at 298 K.

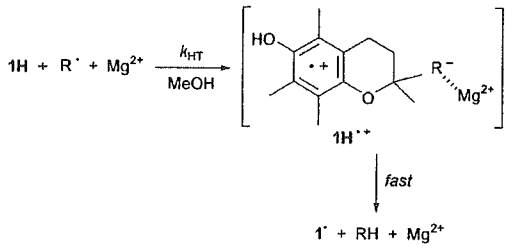


**Scheme 1** Radical-scavenging reaction by **1H** *via* an electron transfer in MeOH.

the coordination of $Mg^{2+}$ to DPPH$^-$ or GO$^-$ may stabilize the product, resulting in the acceleration of the electron transfer.

### Effect of base on the rates of radical scavenging reactions

In protic media, such as alcohols and water, **1H** may be in equilibrium with the corresponding phenolate anion **1**$^-$, which is a much stronger electron donor as compared to the parent **1H**.[20] In such a case, **1**$^-$ may act as an electron donor rather than the parent **1H** in MeOH.

In order to clarify an actual electron donor in MeOH, the effect of base on the radical-scavenging rates of **1H** was examined. The addition of pyridine to the **1H**–DPPH$^{\cdot}$ system results in a significant increase in the rate of the DPPH$^{\cdot}$-scavenging reaction by **1H**. The $k_{HT}$ value increases with increasing pyridine concentration to reach a constant value as shown in Fig. 2. When pyridine is replaced by 2,6-lutidine, a stronger base than pyridine, the limiting $k_{HT}$ value is larger than that in the case of pyridine, as shown in Fig. 2. If the rate of acceleration is due to the deprotonation of the phenolic OH group of **1H** in the presence of base, the limiting $k_{HT}$ value should be the same regardless of the basicity of pyridines. The different limiting $k_{HT}$ values between pyridine and 2,6-lutidine in Fig. 2 suggest that little deprotonation occurs to produce **1**$^-$ and that the actual electron donor is the parent **1H** rather than **1**$^-$ in MeOH, as shown in Scheme 1. In such a case, the coordination of pyridines

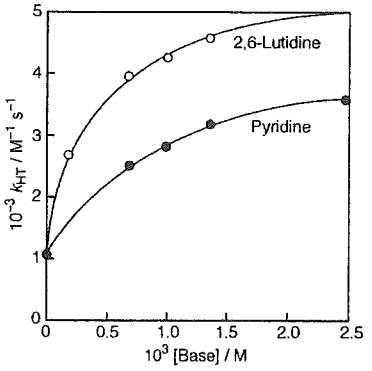


**Fig. 2** Plot of $k_{HT}$ *vs.* [base] for the reaction of **1H** with DPPH$^{\cdot}$ in the presence of pyridine (black circles) or 2,6-lutidine (white circles) in de-aerated MeOH at 298 K.

to **1H**$^{\cdot+}$ may stabilize the product, resulting in the acceleration of the initial electron-transfer process. In the presence of a large amount of a strong Lewis acid, such as $Mg(ClO_4)_2$, no deprotonation of **1H** occurs in MeOH.

### Solvent effect on the one-electron oxidation potential of the vitamin E model

The solvent effect on the one-electron oxidation potential ($E^0_{ox}$) of **1H** was examined by cyclic voltammetry (CV) and second-harmonic alternating current voltammetry (SHACV) measurements.[11–16] Very recently, Williams and Webster have reported that the one-electron oxidation of α-tocopherol itself occurs at about 0.97 V *vs.* SCE in MeCN (0.25 M $Bu_4NPF_6$) based on the detailed electrochemical analyses.[21] A similar cyclic voltammogram was observed for the electrochemical oxidation of **1H** in MeCN (0.1 M $Bu_4NClO_4$) (data not shown), from which was determined the $E^0_{ox}$ value (*vs.* SCE) of **1H** in MeCN as 0.97 V. On the other hand, the CV wave of **1H** in MeOH (0.1 M $Bu_4NClO_4$) was irreversible. Thus, SHACV measurement was carried out to determine the $E^0_{ox}$ value of **1H** in MeOH. The $E^0_{ox}$ value (*vs.* SCE) of **1H** in MeOH (0.1 M $Bu_4NClO_4$), determined from the intersection of an SHACV wave (Fig. 3), is located at 0.63 V, which is significantly more negative than the value in MeCN (0.97 V). Such a negative shift of the $E^0_{ox}$ value in MeOH as compared to that in MeCN may be ascribed to a stronger solvation of **1H**$^{\cdot+}$ in MeOH than in MeCN. Thus, the ease of one-electron oxidation of **1H** in MeOH as compared to in MeCN may result in the difference in the radical-scavenging mechanism.

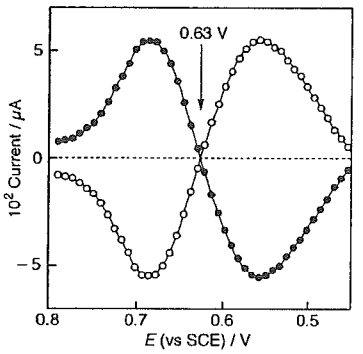


**Fig. 3** SHACV of **1H** recorded at the scan rate of 4 mV $s^{-1}$ on Pt working electrode in de-aerated MeOH (0.1 M $Bu_4NClO_4$) at 298 K.

### EPR spectrum of the phenoxyl radical derived from the vitamin E model in de-aerated MeOH

The EPR detection of radical species derived from **1H** would provide valuable information about the solvation of the radical species.[22,23] The EPR spectrum of **1**$^{\cdot}$ in de-aerated MeOH at 298 K is shown in Fig. 4a. It should be noted that the *g* value of the EPR spectrum of **1**$^{\cdot}$ in MeOH (2.0040) is apparently smaller than that in MeCN (2.0047).[7] The observed hyperfine structure in Fig. 4a is well reproduced by the computer simulation (Fig. 4b) with four hyperfine splitting constants (*hfc*) listed in Table 1. Table 1 also shows the *hfc* values of **1**$^{\cdot}$ in MeCN.[7] All the *hfc* values in MeOH are also smaller than those in MeCN. The smaller *g* value of the EPR spectrum of **1**$^{\cdot}$ as well as the smaller *hfc* values in MeOH than those in MeCN indicates that the stronger solvation of **1**$^{\cdot}$ may occur in MeOH than in MeCN. Although the EPR spectrum of **1H**$^{\cdot+}$ could not be observed because of the fast deprotonation to produce **1**$^{\cdot}$ (Scheme 1), stronger solvation of **1H**$^{\cdot+}$ may also occur in MeOH than in MeCN, resulting in the ease of one-electron oxidation of **1H** in MeOH than in MeCN.

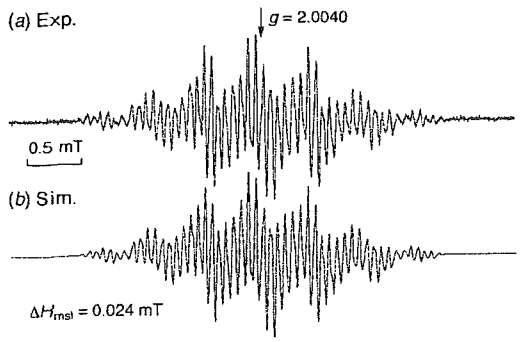


**Fig. 4** (a) EPR spectrum of **1**$^{\cdot}$ generated in the reaction of **1H** ($1.0 \times 10^{-3}$ M) with DPPH$^{\cdot}$ ($2.0 \times 10^{-4}$ M) in de-aerated MeOH at 298 K. (b) The computer simulation spectrum. The *hfc* values used for the simulation are listed in Table 1.

**Table 1** Hyperfine splitting constants (*hfc*; in mT) and *g* values of **1**$^{\cdot}$ in de-aerated solvents

| Solvent | *g* | $a(3H^5)$ | $a(3H^7)$ | $a(3H^8)$ | $a(2H^4)$ |
|---|---|---|---|---|---|
| MeOH | 2.0040 | 0.577 | 0.423 | 0.073 | 0.126 |
| MeCN | 2.0047[a] | 0.587[a] | 0.440[a] | 0.086[a] | 0.139[a] |

[a] Taken from ref. 7.

In conclusion, the scavenging reaction of DPPH$^{\cdot}$ or GO$^{\cdot}$ by **1H** in MeOH proceeds *via* the electron transfer from **1H** to DPPH$^{\cdot}$ or GO$^{\cdot}$ followed by proton transfer rather than *via* the one-step hydrogen atom transfer, which has been observed in MeCN. Such a difference in the mechanism of radical-scavenging reactions by the vitamin E model depending on the solvents provides valuable information for the biological antioxidative reactions.

## Acknowledgements

This work was partially supported by a Grant-in-Aid for Scientific Research (A) (No. 16205020) and a Grant-in-Aid for Young Scientist (B) (No. 15790032) from the Ministry of Education, Culture, Sports, Science and Technology, Japan.

## References

1 J. S. Wright, E. R. Johnson and G. A. Di Labio, *J. Am. Chem. Soc.*, 2001, **123**, 1173.
2 M. Leopoldini, T. Marino, N. Russo and M. Toscano, *J. Phys. Chem. A*, 2004, **108**, 4916.
3 M. Leopoldini, I. P. Pitarch, N. Russo and M. Toscano, *J. Phys. Chem. A*, 2004, **108**, 92.
4 S. Fukuzumi, in *Electron Transfer in Chemistry*, ed. V. Balzani, Wiley-VCH, New York, 2001, vol. 4, pp. 3–67.
5 I. Nakanishi, K. Miyazaki, T. Shimada, K. Ohkubo, S. Urano, N. Ikota, T. Ozawa, S. Fukuzumi and K. Fukuhara, *J. Phys. Chem. A*, 2002, **106**, 11123.
6 I. Nakanishi, K. Ohkubo, K. Miyazaki, W. Hakamata, S. Urano, T. Ozawa, H. Okuda, S. Fukuzumi, N. Ikota and K. Fukuhara, *Chem. Res. Toxicol.*, 2004, **17**, 26.
7 I. Nakanishi, K. Fukuhara, T. Shimada, K. Ohkubo, Y. Iizuka, K. Inami, M. Mochizuki, S. Urano, S. Itoh, N. Miyata and S. Fukuzumi, *J. Chem. Soc., Perkin Trans. 2*, 2002, 1520.
8 I. Nakanishi, S. Matsumoto, K. Ohkubo, K. Fukuhara, H. Okuda, K. Inami, M. Mochizuki, T. Ozawa, S. Itoh, S. Fukuzumi and N. Ikota, *Bull. Chem. Soc. Jpn.*, 2004, **77**, 1741.
9 H.-Y. Zhang and L.-F. Wang, *J. Phys. Chem. A*, 2003, **107**, 11258.
10 D. D. Perrin, W. L. F. Armarego and D. R. Perrin, *Purification of Laboratory Chemicals, 4th Edition*, Pergamon Press, Elmsford, New York, 1996.
11 T. G. McCord and D. E. Smith, *Anal. Chem.*, 1969, **41**, 1423.
12 A. M. Bond and D. E. Smith, *Anal. Chem.*, 1974, **46**, 1946.
13 M. R. Wasielewski and R. Breslow, *J. Am. Chem. Soc.*, 1976, **98**, 4222.
14 E. M. Arnett, K. Amarnath, N. G. Harvey and J.-P. Cheng, *J. Am. Chem. Soc.*, 1990, **112**, 344.
15 M. Patz, H. Mayr, J. Maruta and S. Fukuzumi, *Angew. Chem., Int. Ed. Engl.*, 1995, **34**, 1225.
16 S. Fukuzumi, N. Satoh, T. Okamoto, K. Yasui, T. Suenobu, Y. Seko, M. Fujitsuka and O. Ito, *J. Am. Chem. Soc.*, 2001, **123**, 7756.
17 K. Mann and K. K. Barnes, in *Electrochemical Reactions in Nonaqueous Systems*, Marcel Dekker Inc., New York, 1990.
18 K. Mukai, Y. Watanabe and K. Ishizu, *Bull. Chem. Soc. Jpn.*, 1986, **59**, 2899.
19 G. Litwinienko and K. U. Ingold, *J. Org. Chem.*, 2003, **68**, 3433.
20 I. Nakanishi, K. Miyazaki, T. Shimada, Y. Iizuka, K. Inami, M. Mochizuki, S. Urano, H. Okuda, T. Ozawa, S. Fukuzumi, N. Ikota and K. Fukuhara, *Org. Biomol. Chem.*, 2003, **1**, 4085.
21 L. L. Williams and R. D. Webster, *J. Am. Chem. Soc.*, 2004, **126**, 12441.
22 T. Yonezawa, T. Kawamura, M. Ushio and Y. Nakao, *Bull. Chem. Soc. Jpn.*, 1970, **43**, 1022.
23 M. Lucarini, V. Mugnaini, G. F. Pedulli and M. Guerra, *J. Am. Chem. Soc.*, 2003, **125**, 8318.

J|A|C|S
ARTICLES
Published on Web 07/28/2005

# Photoinduced Nitric Oxide Release from Nitrobenzene Derivatives

Takayoshi Suzuki,† Osamu Nagae,† Yuka Kato,† Hidehiko Nakagawa,† Kiyoshi Fukuhara,‡ and Naoki Miyata*,†

*Contribution from the Graduate School of Pharmaceutical Sciences, Nagoya City University, 3-1 Tanabe-dori, Mizuho-ku, Nagoya, Aichi 467-8603, Japan, and the Division of Organic Chemistry, National Institute of Health Sciences, Setagaya, Tokyo 158-8501, Japan*

Received February 25, 2005; E-mail: miyata-n@phar.nagoya-cu.ac.jp

***Abstract:*** A new type of photoinduced nitric oxide (NO) donors was designed from nitrobenzene derivatives. Visible-light irradiation of 2,6-dimethylnitrobenzenes bearing extended $\pi$-electron systems at the 4-position revealed efficient NO release using ESR analysis and the Griess assay. Computational study and ultraviolet spectrum analysis suggested that the NO-releasing activity was closely related to the conformation of the nitro group, the absorption intensity, and the length of the conjugated $\pi$-electron system. Employing the photodependent cytotoxicity of compound **14** against HCT116 human colon cancer cells, it was demonstrated that 4-substituted-2,6-dimethylnitrobenzene analogues are useful NO donors for the time- and site-controlled NO treatment.

## Introduction

Nitric oxide (NO), a simple diatomic free radical, has proven in recent years to be involved in the maintenance and regulation of vital functions[1] and is one of the most fascinating and studied compounds in biological chemistry, although for decades it was merely viewed as an environmental pollutant. The development and use of NO donors have played important roles in research on NO physiology,[2] and the significance of these donors has recently been reaffirmed not only from the perspective of reagents for biological studies but also with a view to their application as pharmaceuticals.[3] To date, a number of NO donors have been developed[2,4] and utilized. However, many of the currently used NO donors such as 1-hydroxy-2-oxo-3-(aminoalkyl)-1-triazenes (NOCs)[5] and 4-alkyl-2-hydroxyimino-5-nitro-3-hexenes (NORs)[6] are reagents that release NO by spontaneous autolysis. For further research on NO physiology and potential therapeutic application, it appeared desirable to liberate NO in living systems in a time- and site-controlled manner. This concept led to the identification of several photochemically triggered NO donors such as metal nitrosyl compounds[7] and some caged nitric oxides.[8] The duration and site of NO release from these compounds can be controlled by changing the interval and position of light exposure. However, some of these photoinducible NO donors have problems associated with stability and toxicity. For example, the NO-releasing rate of metal nitrosyl compounds such as dipotassium pentachloronitrosylruthenate and sodium nitroprusside (SNP) varies with changes in pH, and SNP has toxic consequences attributable to the cyanide ligand.[9]

We previously found 6-nitrobenzo[*a*]pyrene (6-nitroBaP) (Figure 1) to be a photoinducible NO-releasing agent[10] whose NO-releasing mechanism is completely different from those of well-known photochemically triggered NO donors. 6-NitroBaP releases NO with the concomitant formation of 6-oxylBaP radical under visible-light irradiation (Figure 1). Based on the fact that 1-nitroBaP and 3-nitroBaP with sterically less hindered nitro

† Nagoya City University.
‡ National Institute of Health Sciences.

(1) (a) Ignarro, L. J.; Buga, G. M.; Wood, K. S.; Byrns, R. E.; Chaudhuri, G. *Proc. Natl. Acad. Sci. U.S.A.* **1987**, *84*, 9265−9269. (b) Palmer, R. M.; Ferige, A. G.; Moncada, S. *Nature* **1987**, *327*, 524−526. (c) Stamler, J. S.; Singel, D. J.; Loscalzo, J. *Science* **1992**, *258*, 1898−1902.
(2) For a review, see: Wang, P. G.; Xian, M.; Tang, X.; Wu, X.; Wen, Z.; Cai, T.; Janczuk, A. J. *Chem. Rev.* **2002**, *102*, 1091−1134.
(3) (a) Janero, D. R.; Ewing, J. F. *Free Radical Biol. Med.* **2000**, *29*, 1199−1221. (b) Buergler, J. M.; Tio, F. O.; Schulz, D. G.; Khan, M. M.; Mazur, W.; French, B. A.; Raizner, A. E.; Ali, N. M. *Coron. Artery Dis.* **2000**, *11*, 351−357.
(4) (a) For a review, see: McCleverty, J. A. *Chem. Rev.* **2004**, *104*, 403−418. (b) For a review, see: Ohwada, T.; Uchiyama, M. *J. Synth. Org. Chem. Jpn.* **2003**, *61*, 47−59.
(5) (a) Maragos, C. M.; Morley, D.; Wink, D. A.; Dunams, T. M.; Saavedra, J. E.; Hoffmann, A.; Bove, A. A.; Isaac, L.; Hrabie, J. A.; Keefer, L. K. *J. Med. Chem.* **1991**, *34*, 3242−3247. (b) Hrabie, J. A.; Klose, J. R.; Wink, D. A.; Keefer, L. K. *J. Org. Chem.* **1993**, *58*, 1472−1476. (c) Saavedra, J. E.; Shami, P. J.; Wang, L. Y.; Davies, K. M.; Booth, M. N.; Citro, M. L.; Keefer, L. K. *J. Med. Chem.* **2000**, *43*, 261−269. (d) Davies, K. M.; Wink, D. A.; Saavedra, J. E.; Keefer, L. K. *J. Am. Chem. Soc.* **2001**, *123*, 5473−5481.
(6) (a) Thomas, G.; Ramwell, P. W. *Biochem. Biophys. Res. Commun.* **1989**, *164*, 889−893. (b) Kato, M.; Nishino, S.; Ohno, M.; Fukuyama, S.; Kita, Y.; Hirasawa, Y.; Nakanishi, I.; Takasugi, H.; Sakane, K. *Bioorg. Med. Chem. Lett.* **1996**, *6*, 33−38. (c) Fukuyama, S.; Hirasawa, Y.; Kato, Y.; Nishino, S.; Macda, K.; Kato, M.; Kita, Y. *J. Pharmacol. Exp. Ther.* **1997**, *282*, 236−242.
(7) Flitney, F. W.; Megson, I. L.; Flitney, D. E.; Butler, A. R. *Br. J. Pharmacol.* **1992**, *107*, 842−848.
(8) (a) Makings, L. R.; Tsien, R. Y. *J. Biol. Chem.* **1994**, *269*, 6282−6285. (b) Kwon, N. S.; Lee, S. H.; Choi, C. S.; Kho, T.; Lee, H. S. *FASEB J.* **1994**, *8*, 529−533. (c) Singh, R. J.; Hogg, N.; Joseph, J.; Kalyanaraman, B. *FEBS Lett.* **1995**, *360*, 47−51. (d) Namiki, S.; Arai, T.; Fujimori, K. *J. Am. Chem. Soc.* **1997**, *119*, 3840−3841. (e) Namiki, S.; Kaneda, F.; Ikegami, M.; Arai, T.; Fujimori, K.; Asada, S.; Hama, H.; Kasuya, Y.; Goto, K. *Bioorg. Med. Chem.* **1999**, *7*, 1695−1702.
(9) Shishido-Silvia, M.; Ganzarolli de Oliveira, M. *Prog. React. Kinet.* **2001**, *26*, 239−261.
(10) Fukuhara, K.; Kurihara, M.; Miyata, N. *J. Am. Chem. Soc.* **2001**, *123*, 8662−8666.


10.1021/ja0512024 CCC: $30.25 